



This is a repository copy of *Bioengineering vascular networks to study angiogenesis and vascularisation of physiologically relevant tissue models in vitro*.

White Rose Research Online URL for this paper:
<https://eprints.whiterose.ac.uk/160448/>

Version: Published Version

Article:

Dikici, S. orcid.org/0000-0001-9933-5254, Claeysens, F. orcid.org/0000-0002-1030-939X and MacNeil, S. orcid.org/0000-0002-9188-5769 (2020) Bioengineering vascular networks to study angiogenesis and vascularisation of physiologically relevant tissue models in vitro. ACS Biomaterials Science & Engineering, 6 (6). pp. 3513-3528. ISSN 2373-9878

<https://doi.org/10.1021/acsbomaterials.0c00191>

Reuse

This article is distributed under the terms of the Creative Commons Attribution (CC BY) licence. This licence allows you to distribute, remix, tweak, and build upon the work, even commercially, as long as you credit the authors for the original work. More information and the full terms of the licence here:
<https://creativecommons.org/licenses/>

Takedown

If you consider content in White Rose Research Online to be in breach of UK law, please notify us by emailing eprints@whiterose.ac.uk including the URL of the record and the reason for the withdrawal request.



eprints@whiterose.ac.uk
<https://eprints.whiterose.ac.uk/>

Bioengineering Vascular Networks to Study Angiogenesis and Vascularization of Physiologically Relevant Tissue Models *in Vitro*

Serkan Dikici, Frederik Claeysens, and Sheila MacNeil*

Cite This: *ACS Biomater. Sci. Eng.* 2020, 6, 3513–3528

Read Online

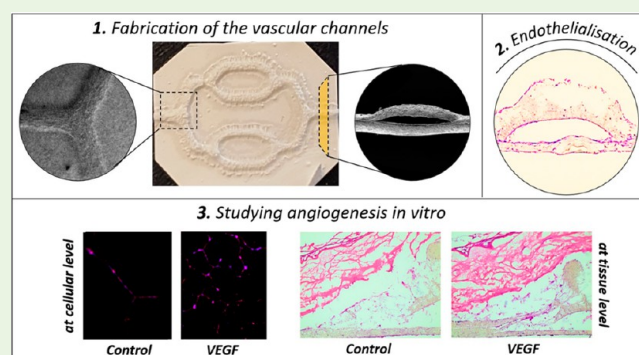
ACCESS |

Metrics & More

Article Recommendations

ABSTRACT: Angiogenesis assays are essential for studying aspects of neovascularization and angiogenesis and investigating drugs that stimulate or inhibit angiogenesis. To date, there are several *in vitro* and *in vivo* angiogenesis assays that are used for studying different aspects of angiogenesis. Although *in vivo* assays are the most representative of native angiogenesis, they raise ethical questions, require considerable technical skills, and are expensive. *In vitro* assays are inexpensive and easier to perform, but the majority of them are only two-dimensional cell monolayers which lack the physiological relevance of three-dimensional structures. Thus, it is important to look for alternative platforms to study angiogenesis under more physiologically relevant conditions *in vitro*. Accordingly, in this study, we developed polymeric vascular networks to be used to study angiogenesis and vascularization of a 3D human skin model *in vitro*. Our results showed that this platform allowed the study of more than one aspect of angiogenesis, endothelial migration and tube formation, *in vitro* when combined with Matrigel. We successfully reconstructed a human skin model, as a representative of a physiologically relevant and complex structure, and assessed the suitability of the developed *in vitro* platform for studying endothelialization of the tissue-engineered skin model.

KEYWORDS: angiogenesis, vascularization, 3D model, angiogenesis model, tissue engineering, skin, tissue-engineered skin model



1. INTRODUCTION

Angiogenesis is a sophisticated process regulated by a complex web of interactions of endothelial cells (ECs) with their extracellular matrix (ECM) and with biochemical and mechanical factors.¹ The delayed neovascularization of tissue-engineered (TE) constructs postimplantation can cause them to fail clinically.² Thus, investigating the factors that regulate angiogenesis is particularly important to understand how they are involved in this complex process.

Angiogenesis assays are powerful tools to study aspects of angiogenesis and can be categorized into three main categories: (i) *in vitro*, (ii) *ex vivo*, and (i) *in vivo*.³ *In vivo* assays are the most representative of native angiogenesis, but since healthy animals are used to perform these assays, they are ethically questionable, require considerable technical skills, and expensive.⁴ In contrast, *in vitro* assays are inexpensive and relatively easy to perform. However, the majority of them are based on two-dimensional (2D) cell culture systems which lack the physiological relevance that three-dimensional (3D) structures can provide.⁵ Thus, it is important to develop better *in vitro* platforms that enable the study of angiogenesis under more physiologically relevant conditions.

Several *in vitro* angiogenesis models fabricated by combining several methods including Bio-MEMS,⁶ 3D printing and porogen leaching,^{7,8} 3D printing, and electrospinning^{9,10} have previously been reported. However, most of them rely on the use of natural gels and allow the evaluation of angiogenesis at only the cellular level. Although these natural gels are biologically preferable by endothelial cells in terms of providing an improved cell attachment, proliferation, and sprouting,¹¹ the use of natural materials limits control over degradability, formability, and mechanical properties.

Skin is the largest organ in the body and acts as a physical barrier between the body and the external environment. It is composed of histologically definable three main layers: the epidermis, the dermis, and the hypodermis. In the cellular level, keratinocytes are the most common type of cells located in the epidermal layer of the skin, and they form different

Received: February 6, 2020

Accepted: April 29, 2020

Published: April 29, 2020



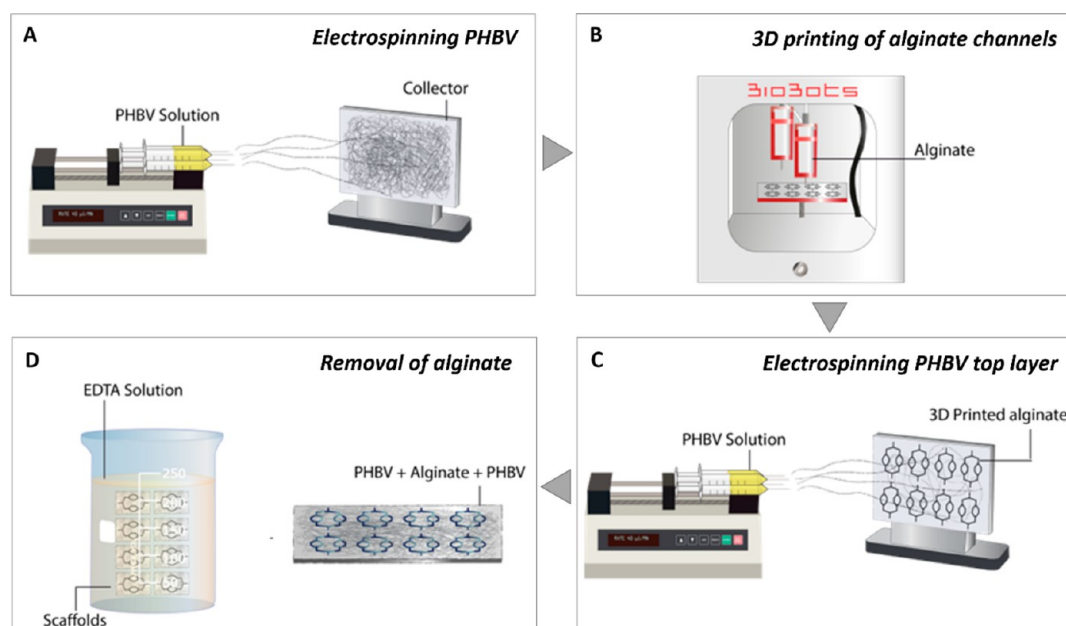


Figure 1. Schematic illustration showing the four-step manufacturing process of synthetic vascular channels. (A) Electrospinning PHBV, (B) 3D printing of the sacrificial alginate channels, (C) electrospinning another layer of PHBV on top of alginate channels, and (D) removal of alginate.

layers of the epidermis with different tasks. Fibroblasts, the second common type of cells in skin, are located in the dermal layer and provide physical strength as well as elasticity of skin.^{12,13} Skin tissue engineering has gained great momentum over the years. However, developing biologically relevant *in vitro* tissue models as alternatives to animal models or as physiologically relevant tissue substitutes for clinical use is always open for improvement.

Several *in vitro* skin models have been developed by many groups or companies over the years to study different subjects such as being alternatives to animal testing, wound healing, pigmentation, contraction, tumor invasion, barrier function, and bacterial infection studies.^{12,14} Facy et al. created a reconstructed epidermis model with Langerhans cells and used this model to test the reactivity of these cells to known allergens and UV.¹⁵ Kandarova et al. studied skin irritation using two reconstructed human skin equivalents as an alternative to animal testing.¹⁶ To study pigmentation, Bessous et al. developed an *in vitro* reconstructed epidermis using autologous keratinocytes and melanocytes.¹⁷ Meier et al. developed a human skin equivalent to study melanoma progression, and they reported a close correspondence between the growth of melanoma into engineered skin construct and *in vivo*.¹⁸ Admane et al. reported the direct 3D bioprinting of full-thickness skin constructs that mimics the signaling pathways of skin.¹⁹ Similarly, Kim et al. developed a 3D printed skin model with perfusable vascular channels to create a vascularized skin model.²⁰ Kolesky et al. developed a platform using a multimaterial 3D bioprinting method, which enables researchers to create thick tissue models with engineered matrix and embedded vasculature.²¹ Recently, John et al. demonstrated the regeneration of TE skin substitute on human amniotic membrane.²² Our laboratory has previously reported a 14 day protocol for the reconstruction of a 3D human skin model that is suitable for clinical use²³ and have previously explored adding human dermal microvascular endothelial cells (HDMECs) to the TE skin model with very little success—the cells struggled to enter the TE skin and

showed no signs of being organized when they did enter.²⁴ Although TE skin was being studied for a long time to be used as skin substitutes in the clinic or *in vitro* models for research, the main challenge remains the same: studying and improving angiogenesis/vascularization of a TE skin for translation of it to clinic or for doing research on understanding the basic principles of skin vascularization. Either for implanting or for *in vitro* laboratory research, developing a vascularized 3D human skin model is highly important for the successful take of TE skin substitute after implantation or studying the effect of chemical, mechanical, and environmental factors on neo-vascularization of skin. Thus, there is a need to develop new platforms that enable the study of vascularization of complex tissues such as skin.

Accordingly, in this study, we fabricated synthetic vascular networks (SVNs) made of poly-3-hydroxybutyrate-co-3-hydroxyvalerate (PHBV), a biocompatible and biodegradable polyester, combining electrospinning and 3D printing techniques to study angiogenesis in a physiologically more relevant environment and to investigate the vascularization of a reconstructed human skin model. The main aim of this study was to create a unique *in vitro* platform that enables researchers to study more than one aspect of angiogenesis at both cellular and tissue levels. PHBV channels were used as physical support and a structural guide for ECs to create a preformed endothelium-like structure. This endothelium-like structure was then used to study the migratory response and tube-forming capability of ECs in response to proangiogenic agents *in vitro* and to explore how synthetic channels can be used as a model for the vascularization studies at the tissue level. The chick chorioallantoic membrane (CAM) assay has been used for the first time as a surrogate for a well-vascularized wound bed to provide the source of blood vessels to grow into the 3D human skin as a positive control to the PHBV SVN vascularization studies.

2. EXPERIMENTAL SECTION

2.1. Materials. 2-Deoxy-D-ribose (2dDR), 37% formaldehyde (FA) solution, 4',6-diamidino-2-phenylindole (DAPI) solution, adenine, AlamarBlue cell metabolic activity assay, alginate sodium salt, amphoterin B, anti-CD31 (PECAM-1) antibody produced in mouse, bovine serum albumin (BSA), calcium chloride dihydrate, chlorotoxin, collagenase A, D-glucose, dimethyl sulfoxide (DMSO), Dulbecco's modified Eagle's medium (DMEM), ethylenediaminetetraacetic acid (EDTA), eosin Y solution, ethanol, F-12 HAM nutrient mixture, fetal calf serum (FCS), fibrinogen from human plasma, glutaraldehyde (25%), glycerol, hematoxylin solution, hydrocortisone, insulin (human recombinant), L-glutamine, methylene blue, penicillin/streptomycin, phalloidin, fluorescein isothiocyanate (FITC), phalloidin, tetramethylrhodamine isothiocyanate (TRITC), sodium hydroxide pellets, Trypan blue, trypsin EDTA, Tween20, vascular endothelial growth factor (VEGF), and sodium chloride (NaCl) were purchased from Sigma-Aldrich. Dichloromethane (DCM), DPX mounting medium, industrial methylated spirit (IMS), methanol, Triton X-100, and xylene were purchased from Fisher Scientific. Human dermal microvascular endothelial cells (HDMECs), endothelial cell growth medium MV (EC GM), and EC GM microvascular (MV) supplement pack were purchased from PromoCell. CellTracker Green, CellTracker Red, and Alexa Fluor 546 Goat anti-Human IgG (H+L) cross-adsorbed secondary antibody were purchased from ThermoFisher. Poly-3-hydroxybutyrate-co-3-hydroxyvalerate (12%) (PHBV) was purchased from GoodFellow. Matrigel (growth factor reduced) was purchased from Corning. Thrombin (human) was purchased from Cayman Chemical. Epidermal growth factor (EGF) was purchased from R&D systems. Optimum cutting temperature tissue freezing medium (OCT-TFM) was purchased from Leica Biosystems.

2.2. Methods. **2.2.1. Manufacturing of the SVN Made of PHBV.** The channels of the SVN were designed using computer-aided design (CAD) software (SolidWorks 2012, Waltham, MA). Following the 3D design of SVN channels, scaffolds were manufactured via the four-step process, as shown by Figure 1.

Alginate was then used as a sacrificial substrate and 3D printed on to PHBV using a 3D bioprinter (BioBots, Philadelphia, PA). Following that, another layer of PHBV was electrospun on top of the alginate using same parameters. Finally, alginate was removed via EDTA solution.

2.2.1.1. Electrospinning PHBV. First, PHBV (10% (w/w)) granules were dissolved in DCM:methanol (90:10 w/w) solvent blend in a fume hood. PHBV polymer solution (~5 mL) was loaded into 5 mL syringes fitted with 0.6 mm inner diameter syringe tips. Syringes were then placed in a syringe pump (GenieTMPlus, KentScientific, Torrington, CT). Aluminum foil was used as the collector and placed at a distance of 17 cm from the needle tips. The pump was set to 40 $\mu\text{L}/\text{min}$, and 17 kV voltage was applied to both the collector and the tips. The polymer was electrospun on the collector with the parameters given above for 1 h.

2.2.1.2. 3D Printing of Alginate as a Sacrificial Material. 1.5% alginate paste was produced by dissolving 0.2 g of calcium chloride dihydrate ($\text{CaCl}_2 \cdot 2\text{H}_2\text{O}$) into 72.7 g of distilled water (dH_2O) while continuously stirring using a magnetic stirrer. The solution was then heated to approximately 60 $^\circ\text{C}$ before adding 1.5 g of alginate sodium salt while continuously stirring on a hot plate magnetic stirrer. Once it was fully dissolved and dehydrated, 24.25 g of glycerol was added and stirred until a smooth viscous paste was obtained.

Prior to 3D printing, the desired numbers of 3D models were oriented and sliced using g-code generator software (Repetier-Host, Willich, Germany). The model was then exported as g-code using the following parameters: 0.4 mm layer height, 0.4 mm nozzle diameter, and 2 mm/s speed. The alginate paste was transferred into a 10 mL syringe with 0.4 mm blunt tip, and the syringe was inserted to the extruder of the 3D bioprinter. The aluminum foil containing the electrospun PHBV layer was placed onto the lid of a 6-well plate and fixed using adhesive paper tape. G-code was then uploaded to the 3D printing software (Bioprint, Philadelphia, PA), and the pressure was

adjusted between 11 and 20 psi. Finally, the extruders were calibrated, and the alginate was 3D printed on the PHBV electrospun sheet. Following the 3D printing process, the electrospinning process was repeated using the same parameters to create synthetic vascular channels inside two layers of PHBV.

2.2.1.3. Removal of Alginate. 0.5 M EDTA solution was prepared in dH_2O . The pH was then adjusted to 8.0 by adding sodium hydroxide (NaOH) beads while stirring continuously.

The scaffolds were submerged in 0.5 M EDTA solution overnight on a shaker (Fisher Scientific, Waltham, MA) set to 70 oscillations/min to create hollow channels between two layers of PHBV sheets by removing alginate. Two ends of the scaffolds were cut to allow alginate to be removed prior to submerging it into EDTA solution.

2.2.2. Characterization of the PHBV SVN. **2.2.2.1. Scanning Electron Microscopy (SEM).** The surface morphology and the cross sections of PHBV SVN were observed under SEM (Philips/FEI XL-20 SEM; Cambridge, UK). The samples were coated with gold using a gold sputter (Edwards sputter coater S150B, Crawley, England) prior to imaging. Average fiber diameter and pore size were measured using ImageJ software (Wayne Rasband, National Institutes of Health) as described previously.²⁵

2.2.2.2. Biomechanical Testing of PHBV SVN. Tensile testing was carried out for the dry and wet scaffolds using a uniaxial mechanical testing machine (BOSE Electroforce Test Instruments, Eden Prairie, MN) equipped with a 22 N load cell. Scaffolds were submerged in PBS for 1 h before testing to be wetted. The clamps of the device were positioned 15 mm away from each other, and the width and thickness of each scaffold were measured. Test samples either dry or wet were clamped with two grips in a tensiometer. Tensile tests were performed on each sample at a rate of 0.1 mm/s until the samples fail. The raw data of the tests were taken and tabulated before converting them into stress–strain curves. Stress and strain values were calculated using eqs 1 and 2:

$$\text{stress (MPa)} = \frac{\text{force (N)}}{\text{area (mm}^2\text{)}} \quad (1)$$

$$\text{strain} = \frac{\text{length of stretch (mm)}}{\text{original length (mm)}} \quad (2)$$

Ultimate tensile strength (UTS), yield strength (YS), and stiffness parameters were calculated using stress (σ) and strain (ϵ) curves of each sample.

Suture retention tests were performed based on the BS EN ISO 7198:2017, which is the standard for testing vascular grafts and patches. Before clamping the samples to a uniaxial testing device, scaffolds were sutured from 2 mm away from the upper end with a suture (Ethicon, Bridgewater, NJ) which is for use in general soft tissues. The distance between clamps was then adjusted, and the tests were conducted at a rate of 0.1 mm/s until the samples fail. Suture retention strength was calculated using eq 3:

$$\begin{aligned} \text{suture retention (MPa)} \\ = \frac{\text{suture retention force (N)}}{\text{suture diameter (mm)} \times \text{thickness (mm)}} \quad (3) \end{aligned}$$

2.2.3. Cannulation of the PHBV SVN to Test the Channel Structure and Patency. Prior to cell seeding into PHBV SVN, channels were cannulated with a 25 G cannula by perfusing PBS into the channels under a dissection microscope (Wild Heerbrugg, Heerbrugg, Switzerland). Methylene blue was then injected into channels to visualize the channel structure and patency using a 25 G cannula, and the images of the channels were obtained under a dissection microscope.

2.2.4. Cellularization of Synthetic Scaffolds. For cellularization of the PHBV SVN, two different procedures were assessed: (i) HDMECs were seeded into the channels in isolation, and (ii) HDMECs were seeded into the channels whereas human dermal fibroblasts (HDFs) were seeded to the outer surfaces of the channels.

2.2.4.1. Cellularization of the PHBV Channels with HDMECs in Isolation. The PHBV SVN was disinfected by submerging them in 70% ethanol for 45 min and then washed three times with PBS prior to cell seeding and transferred to Petri dishes. HDMECs were used between passage 2–4. Once they reached 80–90% confluency, 0.5×10^6 HDMECs were resuspended in 0.25 mL of EC GM (supplemented with 2% FCS, 0.4% EC growth supplement, 10 ng/mL EGF, 90 $\mu\text{g}/\text{mL}$ heparin, 1 $\mu\text{g}/\text{mL}$ hydrocortisone) and then perfused into the SVN using a 1 mL syringe with a 25 G cannula. Before adding culture medium, scaffolds were returned to the incubator for 1 h to allow HDMECs to attach to the inside of the channels. Then, 10 mL of HDMEC culture medium was added to each Petri dish, and they were incubated at 37 °C overnight. Scaffolds were flipped over, and the same seeding process was repeated in order to cellularize the other side of the channels on the following day. Scaffolds were kept in culture for 7 days by changing the culture medium every 2–3 days. The PHBV SVN scaffolds were fixed in 3.7% FA. Fixed scaffolds were then embedded in freezing medium and frozen in liquid nitrogen for 3 min. Sections were cut 5–10 μm thick using a cryostat (Leica Biosystems Nussloch, Germany) and stained with hematoxylin and eosin (H&E) as described previously.^{26,27} Briefly, the slides were stained with hematoxylin for 5 min and eosin for 90 s prior to dehydration with serial alcohol washes. The slides were then mounted with DPX mountant and investigated under a light microscope (Motic BA210).

2.2.4.2. Cellularization of the PHBV Channels with HDMECs and HDFs. HDMECs were used between passage 2–4. HDFs were used between passage 2–6, once cells reached 80–90% confluency. The PHBV SVN was disinfected by submerging them in 70% ethanol for 45 min and then washed three times with PBS prior to cell seeding. To be able to image them separately under a fluorescent microscope, each cell type was marked using CellTracker fluorescent probes. To label the HDMECs, 50 μg of CellTracker Red dry powder was dissolved in 7.3 μL of DMSO. Then, 3 mL of serum-free HDMEC culture medium was added to prepare a $\sim 25 \mu\text{M}$ working dye solution. The prewarmed dye solution was then added gently to the T75 flask, and HDMECs were incubated for 1 h under growth conditions. To label the HDFs, 50 μg of CellTracker Green dry powder was dissolved in 10.75 μL of DMSO. Then, 4.3 mL of serum-free HDFs culture medium was added to prepare $\sim 25 \mu\text{M}$ working dye solution. The prewarmed dye solution was then added gently to the T75 flask, and HDFs were incubated for 1 h under growth conditions. Following the labeling of cells, sterile scaffolds were transferred to Petri dishes. 0.5×10^6 HDMECs were trypsinized, centrifuged, and resuspended in 0.25 mL of culture medium and then perfused into the synthetic vascular channels using a 1 mL syringe with 25 G cannula. Following that, 0.5×10^6 HDFs were trypsinized, centrifuged, and resuspended in 200 μL of HDMEC growth medium and pipetted on the outer surface of the channels. Before submerging the scaffolds into HDMEC culture medium, scaffolds were incubated at 37 °C for up to 2 h in order to allow HDFs to be attached on the outer surface. Then, 10 mL of HDMEC culture medium was added to each Petri dish, and they were incubated at 37 °C overnight. Scaffolds were flipped over, and the same CellTracker labeling and seeding protocol was followed in order to cellularize the other side of the channels on the following day. Scaffolds were kept in culture for 7 days by changing the culture medium every 3 days.

In order to verify the presence and check the distribution of the HDMECs within the PHBV vascular channels prior to further experiments, scaffolds were fixed in 3.7% FA, and 5–10 μm thick sections were taken as described in Section 2.2.4.1, immunostained for the expression of CD31, and counterstained with DAPI after the 7 day culture of HDMECs and HDFs in PHBV SVN. Briefly, a hydrophobic barrier pen was used to draw circles around each sample on the slide in order to create a water repellent barrier which creates a reservoir on sections for staining reagents. Cells were permeabilized by incubating in 0.1% Triton-X 100 for 20 min at room temperature (RT) and then in 7.5% BSA at room temperature for 1 h to block unspecific binding of the antibodies. This step was followed by washing once with 1% BSA, and the samples were incubated with the

appropriate primary antibodies diluted in 1% BSA (1:50 dilution was used for anti-CD31 primary antibody) at 4 °C overnight. The next day, samples were washed 3 times with PBS before incubating with the appropriate secondary antibodies diluted in 1% BSA (1:500 dilution is used for AlexaFluor546 conjugated secondary antibody) at RT for 1 h and washing three times with PBS. Samples were counterstained with DAPI solution by incubating for 20 min at RT. Slides were then washed three times with PBS and imaged using a fluorescent microscope (Olympus IX3, Tokyo, Japan).

2.2.5. Fluorescent Staining. For PHBV SVN recellularized with HDMECs in isolation, the scaffolds were fixed in 3.7% FA for 1 h and sectioned using a cryostat as described in Section 2.2.4.1. For analyzing the cells in the PHBV SVN, the sections were stained with phalloidin-TRITC (1:500 diluted in PBS) (or phalloidin-FITC (1:500 diluted in PBS) in some of the experiments) to stain the cytoskeleton. Sections were then stained with DAPI (1:1000 diluted in PBS) to stain cell nuclei. Briefly, 0.1% (v/v) Triton X 100 (in PBS) was added on samples, and the samples were incubated for 20–30 min at room temperature. After three times washing with PBS, either phalloidin solution was added to cells and incubated for 30 min at RT in the dark. Sections were then washed three times with PBS. DAPI solution was then added and incubated for 10–15 min at RT in the dark, and the cells were then washed 3 times with PBS. Finally, DPX mountant was pipetted onto the samples, and samples were covered with a coverslip. Cells were then examined under a fluorescent microscope.

2.2.6. Direct Imaging of Pre-labeled Cells. While investigating HDMECs in coculture with HDFs, cells were pre-labeled using CellTracker fluorescent probes with the intent of distinguishing them during fluorescent imaging. Use of fluorescent probes prior to cultivating cells in the scaffolds enabled us to image HDMECs and HDFs directly under a fluorescent microscope following the sectioning step.

2.2.7. Development of a 3D TE Skin Model. **2.2.7.1. Isolation of Human Foreskin Keratinocytes and HDFs from Skin Grafts.** Skin grafts were obtained from patients who were informed of the use of their skin for research purposes according to a protocol approved by the Sheffield University Hospitals NHS Trust Ethics Committee. Fibroblasts and keratinocytes were isolated from the skin, as described by Ghosh et al.²⁸ Briefly, skin samples were cut into 0.5 cm^2 pieces and incubated overnight in Difco-trypsin (0.1% (w/v) trypsin, 0.1% (w/v) D-glucose in PBS, pH 7.45) before being washed and maintained in PBS.

For isolating keratinocytes, skin samples were taken from the solution and transferred into a Petri dish filled with growth media. The epidermis was peeled off, and the surface of the epidermis (papillary surface) was gently scraped; basal keratinocytes were collected into the growth media. Cells were then harvested by centrifuging at 1000 rpm for 5 min, resuspended and seeded into 75 cm^2 tissue culture flasks with the presence of a feeder layer (irradiated mouse 3T3 (i3T3) cells), and cultured in Green's media (66% DMEM (v/v), 21.6% F12-HAMS (v/v), 10% FCS (v/v), 0.5% insulin, 0.5% adenine, 0.1% T/T, 0.1% chlorotoxin, 0.016% hydrocortisone, 0.01% EGF, 100 IU/mL penicillin, 100 $\mu\text{g}/\text{mL}$ streptomycin, 2 mM L-glutamine, and 0.625 $\mu\text{g}/\text{mL}$ amphotericin B).

HDFs were isolated by mincing the dermis with into 10 mm^2 pieces. The pieces were then incubated overnight at 37 °C in 0.5% (w/v) collagenase A solution. The suspension of fibroblasts was centrifuged at 1000 rpm for 5 min and resuspended in DMEM containing 10% (v/v) FBS, 100 IU/mL penicillin, 100 $\mu\text{g}/\text{mL}$ streptomycin, 2 mM L-glutamine, and 0.625 $\mu\text{g}/\text{mL}$ amphotericin B.

2.2.7.2. Preparation of Acellular De-Epidermized Dermis (DED). DED was prepared from skin grafts according to a modified method described by Chakrabarty et al.²⁹ Briefly, the skin graft was treated in 1 M NaCl solution for 24 h at 37 °C and then washed with PBS for 40 min. The epidermis was removed by peeling off or scraping gently (if the epidermal layer remains, and cells have not been harvested before). DED was kept in Green's media at 37 °C for 2 days to check its sterility.

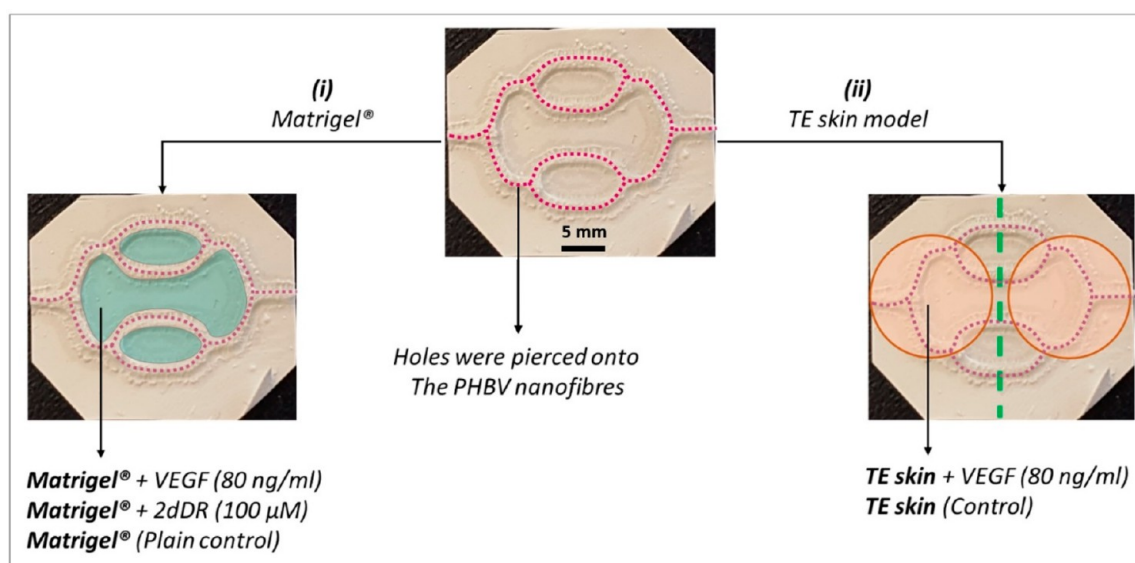


Figure 2. Experiments showing the investigation of the potential of the PHBV SVN to be used as an *in vitro* platform to study angiogenesis and vascularization of a TE skin model. Purple dotted lines represent pierced holes. Matrigel and TE skin are indicated with blue and orange, respectively.

2.2.2.3. Construction of a 3D TE Human Skin Model. A 3D human skin model was reconstructed *in vitro* to study vascularization of the skin using a well-established protocol.²³ Briefly, 1 cm² pieces were cut from DED, and a stainless-steel ring (0.79 cm²) was placed onto the papillary side. HDFs were trypsinized and centrifuged at 1000 rpm for 5 min before being resuspended in DMEM. HDFs (1×10^5) were seeded into the stainless-steel ring and kept in 37 °C while preparing keratinocytes for seeding. The i3T3 feeder layer was removed first using 5 mL of 0.5 M sterile EDTA solution with 3–5 min incubation at 37 °C. After removal of the feeder layer, keratinocytes were then trypsinized and centrifuged at 1000 rpm for 5 min and resuspended in Green's media. HDFs (3×10^5) were seeded into the stainless-steel ring as a coculture with HDFs. TE skin models were incubated overnight at 37 °C before removing the ring and addition of Green's media. 3D skin models were incubated in Green's media for another day (2 days in total), then raised to the air–liquid interface by using a sterile stainless-steel grid, and cultured for a total of 14 days in order to ensure differentiation of the layers of the epidermis.

2.2.8. Use of the PHBV SVN to Study Angiogenesis *In Vitro* and to Investigate the Vascularization of a Reconstructed Skin Model. Two separate experiments were designed to investigate the potential of the developed PHBV SVN to be used as an *in vitro* platform to study angiogenesis and vascularization of a TE skin model: (i) Matrigel outgrowth experiments and (ii) TE skin vascularization studies (Figure 2).

2.2.8.1. Investigating the Endothelial Outgrowth from PHBV Channels to Matrigel. For Matrigel outgrowth experiments, PHBV SVN repopulated with HDMECs (1×10^6 HDMECs per scaffold) were incubated for 7 days as described in Section 2.2.4.1. Once a uniform monolayer of HDMECs was obtained, escape holes were pierced on the channels. The piercing procedure was performed as described previously.³⁰ Approximately 100 equally distanced holes per scaffold were created in random orientations (from top and sides) to cover the surface of all channels as evenly as possible using a sterile 30 G syringe needle. The final concentrations of VEGF and 2dDR within the Matrigel were 80 ng/mL and 1.34 μg/mL, respectively. 100 μL of Matrigel was pipetted into hexagonal wells formed by synthetic channels and 200 μL into the well between two hexagonal wells. Scaffolds were then returned to the incubator for Matrigel to set at 37 °C for 15 min. PHBV scaffolds were then submerged in HDMEC culture medium and cultured for 7 days.

For analyzing the HDMEC outgrowth through Matrigel after culturing HDMECs in the synthetic PHBV vascular scaffolds, the scaffolds were fixed and stained with phalloidin-TRITC and DAPI as described previously. As the scaffolds were opaque and too thick to image directly, they interfered with the visualization of the cellular outgrowth and tube formation when the Matrigel was in place. Thus, the Matrigel was peeled off from the surface of the PHBV SVN, and fluorescent images were taken within the Matrigel close to the edges of the PHBV SVN to investigate the tube formation and the branching. The formation of the tubes can be defined as the gradual formation of capillary-like tubular structures by the ECs in response to proangiogenic stimulants, and connected capillary-like tubes to each other form a meshlike structure within the gel. These meshlike structures are maintained for approximately 24 h. Each closed loop (mostly pentagonal or hexagonal loops) formed by ECs within the gel is defined as a tubelike structure, and the branch sites/nodes are defined as branching points. The number of tubes and branch points are two widely used measures of *in vitro* angiogenesis when conventional tube formation assays are used.³¹ Accordingly, we quantified the total number of tubes and the branch points per field of view as described previously using the Angiogenesis Analyzer plugin of ImageJ³² and AngioTool software,³⁰ respectively.

2.2.8.2. Investigating the Endothelial Outgrowth from PHBV Channels to the Reconstructed Skin Model. For skin vascularization experiments, PHBV synthetic vascular scaffolds populated with HDMECs (1×10^6 HDMECs per scaffold) and HDFs (1×10^6 HDMECs per scaffold) were incubated for 7 days as described in Section 2.2.4.2, and the cellularized scaffolds were then transferred into 6-well plates in a class II biological safety cabinet. Using a sterile 30G syringe needle, holes were pierced on the channels. TE skin models were prepared as described in Section 2.2.7 and cut circular at day 7 prior to implantation. Fibrin glue was used to glue TE skin to PHBV SVN. Use of fibrin glue in skin grafts and TE skin replacements has previously been reported.³³ Fibrin glue was prepared by mixing fibrinogen from human plasma (20 mg/mL in 0.9% NaCl solution in dH₂O) and human thrombin (25 units/mL in 0.1% BSA). Briefly, 50 μL of fibrinogen was pipetted over the surface of the PHBV SVN channels. Then, 50 μL of thrombin was pipetted over fibrinogen, and TE skin models were glued immediately on channels. PHBV scaffolds with TE skin models on them were then submerged in EC GM either supplemented with 80 ng/mL VEGF or nonsupplemented (control) and cultured for a further 7 days at the air–liquid interface. Throughout the experiment duration, EC GM either nonsupple-

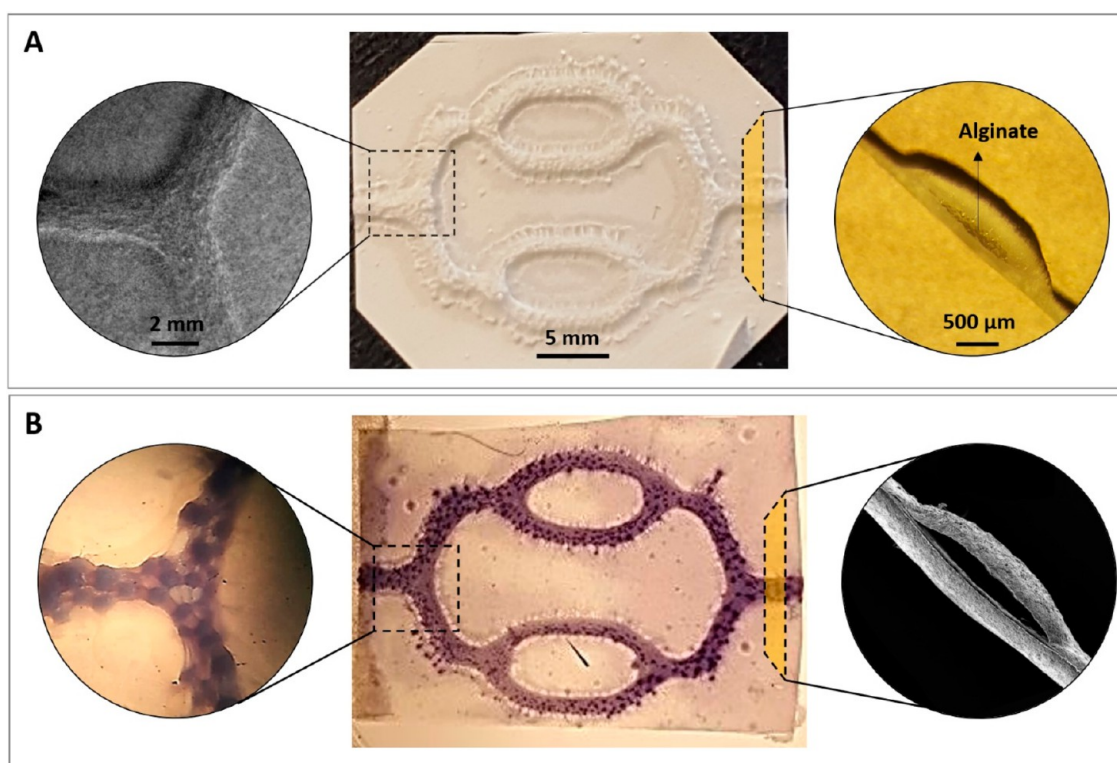


Figure 3. Macrostructure and microstructure of the PHBV SVN scaffolds before and after removal of the 3D printed alginate. (A) Before removal of alginate, SEM images of the channels (top view), macroimage of the PHBV SVN (top view), and dissection microscope image of the cross section of the channels, from left to right, respectively. (B) After removal of alginate, dissection microscope images of the methylene blue injected channels (top view), macroimage of the methylene blue injected PHBV SVN channels (top view), and SEM image of the cross section of the channels, from left to right, respectively.

mented or supplemented with VEGF (80 ng/mL) was pipetted from the top of the TE skin model twice per day.

For the investigation of the HDMEC outgrowth through reconstructed TE skin models, scaffolds with TE skin on top of them were fixed in with 3.7% FA. Fixed PHBV scaffolds with TE skin models were then embedded in OCT freezing medium and frozen in liquid nitrogen for 3 min. The scaffolds were sectioned 5–10 μm thick using a cryostat (Leica Biosystems Nussloch, Germany) at $-20\text{ }^{\circ}\text{C}$ and permeabilized with 0.1% Triton-X100 for 30 min. The sections were then immunostained for anti-CD31 and counterstained with DAPI as described in Section 2.2.4.2. The sections were further investigated histologically by staining the sections with hematoxylin for 1.5 min and eosin for 5 min. The outgrowth distance of HDMECs was determined using ImageJ software, and the results were then statistically analyzed using GraphPad Prism software.

2.2.9. Investigating the Vascularization of the TE 3D Skin Equivalent Using *ex Ovo* CAM Assay. *Ex ovo* CAM assay was used to evaluate the vascularization of the TE skin model as a positive control. A video protocol of *ex ovo* CAM assay has been reported previously by our group.³⁴ Briefly, fertilized chicken eggs (*Gallus domesticus*) were purchased from Henry Stewart & Co. MedEggs (Norwich, UK) and cleaned with 20% IMS solution. Eggs were incubated at $37.5\text{ }^{\circ}\text{C}$ for 3 days in a rocking egg incubator (RCOM King SURO, P&T Poultry, Powys, Wales). On day 3, the embryos were transferred gently into sterile Petri dishes and incubated at $38\text{ }^{\circ}\text{C}$ in a cell culture incubator (Binder, Tuttlingen, Germany). CAM assay was conducted in care of the guidelines of the Home Office, UK. On day 7, reconstructed human skin equivalents (14 day cultured) were cut circular (8 mm diameter) using a biopsy punch and implanted to CAMs for a further 7 days. In order to study the effect of proangiogenic drugs, VEGF and 2dDR were added twice a day dropwise throughout the assay duration. The concentrations of the drugs were 80 ng/day/embryo and 200 μg /day/embryo for VEGF and 2dDR, respectively.

Macroimages of the reconstructed skin equivalents implanted on CAM were taken using a digital USB microscope at embryonic development day 14. Embryos were then euthanized, and the skins were cut with a rim of surrounding CAM tissue and fixed in 3.7% FA solution. Angiogenesis was quantified by counting all blood vessels growing toward the scaffolds in a spoke wheel pattern, as described previously.²⁵ Histological analysis of the samples was performed with H&E staining as described previously in Section 2.2.4.1.

2.2.10. Statistical Analysis. Statistical analysis was carried out using either one-way or two-way analysis of variance (ANOVA) using statistical analysis software (GraphPad Prism, San Diego, CA). Where relevant, *n* values are given in figure captions. Error bars indicate standard deviations in the graphs unless otherwise stated.

3. RESULTS

3.1. Results of the Characterization of the PHBV SVN.

3.1.1. Macrostructure and Microstructure of the PHBV SVN and the Confirmation of the Channel Patency. The combination of electrospinning and 3D printing allowed the production of a number of replicate scaffolds in a short period of time (in less than 2 h). The SEM images of the PHBV SVN showed that it was possible to obtain a connected network of hollow channels after removal of the alginate. The PHBV SVN scaffolds used in this study were approximately ~ 30 mm in length and ~ 18 mm wide with the elongated hexagonal shapes. For each production batch, approximately 12 scaffolds were produced, and 100% of these were used. The macrostructure and the microstructure of the PHBV SVN scaffolds before alginate removal are given in Figure 3A. The removal of alginate was confirmed by the cannulation of the PHBV SVN with methylene blue dye and with the SEM imaging of the

Table 1. Morphological and Mechanical Properties of the PHBV SVN under Dry and Wet Conditions

| | fiber diameter (μm) | pore size (μm) | UTS (MPa) | yield strength (MPa) | stiffness (N/mm) | suture retention (MPa) |
|-----|----------------------------------|-----------------------------|-------------------|----------------------|-------------------|------------------------|
| dry | 0.76 ± 0.22 | 2.73 ± 1.47 | 0.87 ± 0.14^a | 0.58 ± 0.09^b | 6.33 ± 0.59^c | 1.70 ± 0.05^d |
| wet | n/a ^b | n/a | 0.48 ± 0.12^a | 0.12 ± 0.03^b | 0.94 ± 0.14^c | 0.89 ± 0.11^d |

^aa, d: significantly different ($p < 0.05$). b, c: significantly different ($p < 0.005$) ^bn/a = not applicable, $n = 4$.

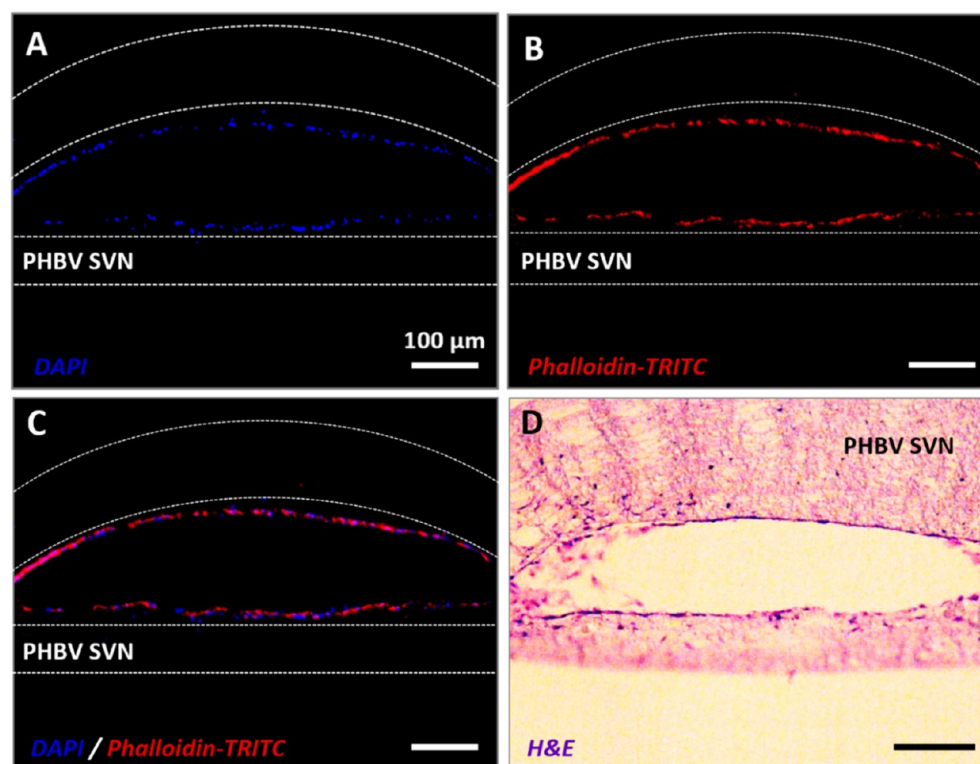


Figure 4. Fluorescent staining of sections taken from scaffolds recellularized with HDMECs in isolation. (A) DAPI (blue), (B) phalloidin-TRITC (red), (C) combined red and blue channels, and (D) H&E staining of the sections from PHBV SVN.

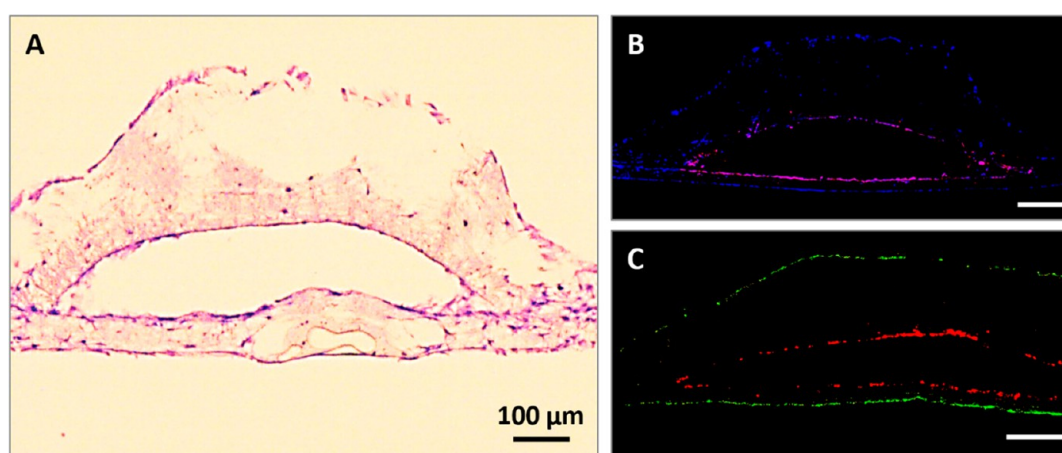


Figure 5. Recellularization of the PHBV SVN with HDMECs and HDFs in indirect contact. (A) H&E staining of the HDMECs inside the channels and HDFs on the outer surface. (B) Immunostained sections of PHBV synthetic vascular scaffolds recellularized with HDMECs within the channels and HDFs on the outer surface. Cell nuclei were stained with DAPI (blue), and CD31+ cells are shown with red. (C) Sections of scaffolds with HDMECs labeled with CellTracker Red inside the channels and HDFs labeled with CellTracker Green on the outer surface of the scaffolds.

open channel structure. The injection of methylene blue through the channels showed that the dye reached all the channels within the network. The highly packed structure of the nanofibrous electrospun fibers allowed the retaining of the dye inside of the channels, and the channels were found open

and interconnected without any leakage between the two layers of PHBV fibers and through small pores between fibers (Figure 3B).

3.1.2. Mechanical Properties of the PHBV SVN. The average diameter of the fibers and the average pore size

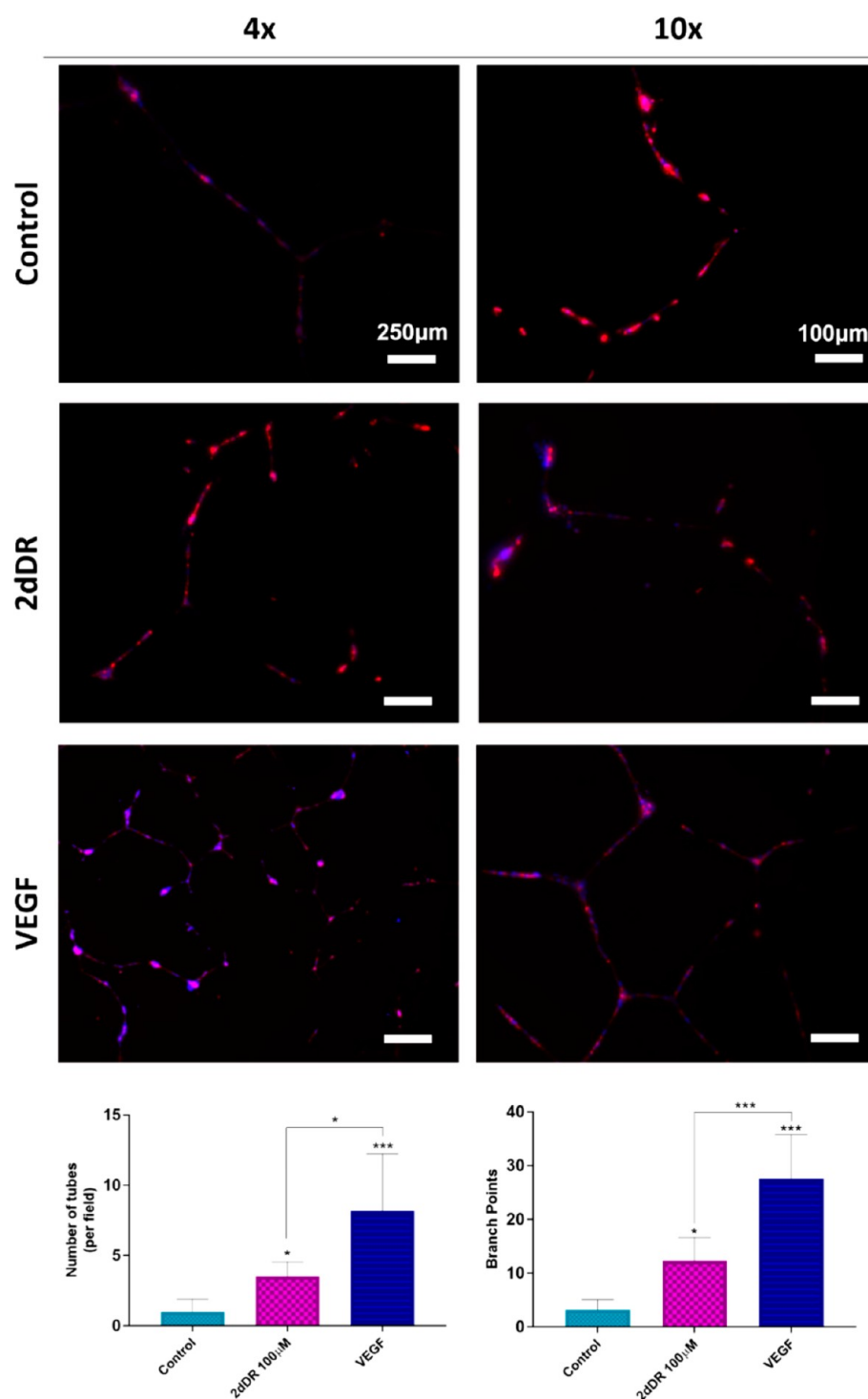


Figure 6. Outgrowing HDMECs from PHBV channels to either plain or VEGF or 2dDR loaded Matrigel. The ECs were stained with phalloidin-TRITC (red) to visualize actin filaments and counterstained with DAPI (blue) to visualize the cell nuclei. Tubelike formed structures were obvious and well-organized in VEGF loaded Matrigel groups when compared with 2dDR loaded and control groups. The graphs show the increase in the number of tubes formed (on the left) and branch points (on the right) within Matrigel when VEGF and 2dDR were loaded (** $p \leq 0.001$, * $p \leq 0.05$).

between the fibers were calculated as 0.76 ± 0.22 and $2.73 \pm 1.47 \mu\text{m}$, respectively. The results of the mechanical testing of the scaffolds showed that the average UTS was higher under dry conditions ($0.87 \pm 0.14 \text{ MPa}$) compared to wet scaffolds ($0.48 \pm 0.12 \text{ MPa}$). The stiffness of the PHBV scaffolds dramatically reduced from 6.33 ± 0.59 to $0.94 \pm 0.14 \text{ N/mm}$ when moistened. Similarly, suture retention of the scaffolds in

the dry state was double that in the wet state (1.70 ± 0.05 and $0.89 \pm 0.11 \text{ MPa}$, respectively, for dry and wet scaffolds). The results of the mechanical tests are summarized in Table 1.

3.1.3. Cellularization of the PHBV SVN with HDMECs in Isolation. To investigate the survival of HDMECs inside the vascular channels without HDFs as supporter cells, HDMECs were seeded inside the PHBV SVN and cultured for 7 days

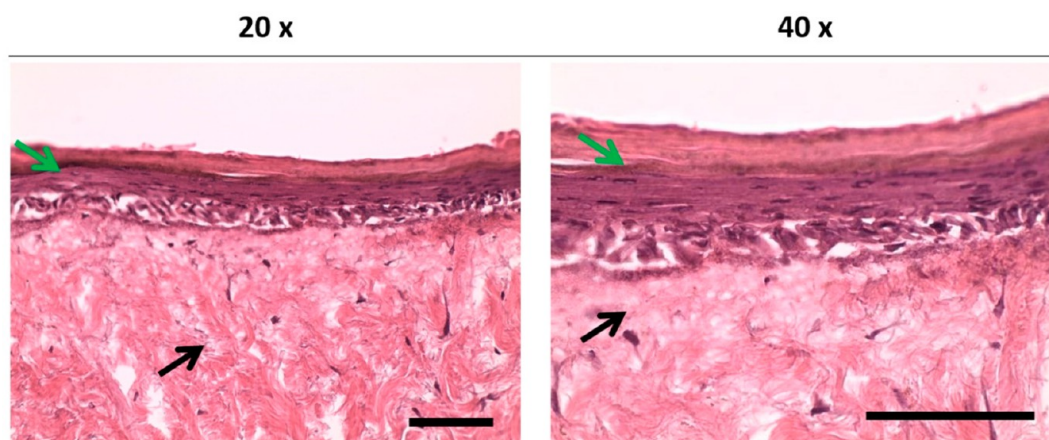


Figure 7. Histological evaluation of the TE skin equivalent models incubated for 2 days in Green's media and then for 12 days at the air–liquid interface. Black and green arrows indicate the dermal layer and differentiated epidermal layers, respectively. Scale bars represent 100 μm .

under static conditions. A complete formation of the HDMEC monolayer within the PHBV SVN has been confirmed with fluorescent and H&E staining (Figure 4).

3.1.4. Cellularization of the PHBV SVN with HDMECs in the Presence of Helper HDFs. To investigate the formation of a continuous EC monolayer inside the synthetic vascular channels, HDMECs were seeded inside the channels in coculture with HDFs on the outer surface. CellTracker labeled and H&E stained images of the sections are given in Figure 5A–C.

Antihuman CD31 (red) stained sections of the PHBV SVN recellularized with HDMECs inside the channels and HDFs on the outer surface cultured over 7 days are given in Figure 5B. The immunostaining showed an evenly distributed HDMEC monolayer within the channels in both curved and flat surfaces, whereas HDFs covering the outer surface of the scaffolds were only stained with DAPI (blue).

3.2. Use of the PHBV SVN to Study Angiogenesis *in Vitro*: Results of HDMEC Outgrowth from PHBV SVN to Matrigel. The results of the Matrigel outgrowth experiments showed that HDMECs were observed as outgrowing and forming interconnected tubelike structures within the Matrigel close to edges of the pierced synthetic PHBV channels by day 7 (Figure 6). Inclusion of both proangiogenic agents, 2dDR and VEGF, increased the formation of tubelike structures. However, tubelike structures were more obvious and well-organized in VEGF loaded Matrigel groups when compared with 2dDR loaded and control groups. Although these experiments were repeated 3 times, and 5 replicates were used for each repeat, it is important to note that the formation of tubelike structures was witnessed in only 20% of the experiments for VEGF loaded Matrigel and 13.3% of the 2dDR loaded and control groups.

The quantification of the fluorescent images showed that inclusion of 2dDR and VEGF in Matrigel increased the number of tubes formed per field within the gel up to 3.5 ± 1.1 and 8.2 ± 4.0 , respectively, where the number of tubes per field was 1.0 ± 0.9 in the control group. Similarly, average branch points were increased from 3.1 ± 1.9 (control) to 12.3 ± 4.4 and 27.6 ± 8.2 , respectively, when 2dDR and VEGF loaded to Matrigel. 80 ng/mL VEGF was found significantly more effective for stimulating tube formation and for increasing branch points when compared to 100 μM 2dDR.

3.3. Use of the PHBV SVN to Study Vascularization of a TE Skin Model.

3.3.1. General Appearance and Histological Evaluation of the 3D TE Skin Models. The macroevaluation of the developed skin model showed that the color of the circular area seeded with HDFs and keratinocytes started to change to a yellowish color which identifies the formation of a new epithelium on DED. The histological evaluation of the reconstructed TE skin models showed that the developed TE skin model achieved a normal-looking gross skin morphology in 14 days. A multilayered epithelium was formed and found to be well attached to the dermis (Figure 7).

3.3.2. Results of the Endothelial Outgrowth from PHBV Channels to 3D TE Skin Model. Following the encouraging results of HDMEC outgrowth through Matrigel, PHBV scaffolds populated with HDMECs and HDFs were investigated for HDMEC outgrowth through the reconstructed TE skin equivalent model.

Immunostained (antihuman CD31) sections showed that HDMECs were evenly distributed within the channels and formed a monolayer, and the outer surface of the PHBV SVN was covered with HDFs (Figure 8). High-magnification images of the immunostained sections revealed that the outgrowing cells from the PHBV channels toward the reconstructed skin models were CD31 positive HDMECs. The outgrowth of HDMECs was mostly observed from the connection edges of two separate electrospun sheets.

The results of the H&E and anti-CD31 staining showed that the addition of VEGF to the growth media significantly increased the outgrowth distance of HDMECs toward the reconstructed TE skin model. The distance of migration went up to $121.7 \pm 6.3 \mu\text{m}$ in the VEGF group when compared to nonsupplemented controls, where the outgrowth distance was $27.9 \pm 11.9 \mu\text{m}$. However, no cellular infiltration to the dermal layer of the implanted skin models was observed in any of the groups.

3.3.3. Results of the Vascularization Study of the TE Skin Model on CAM. In order to assess the effect of the presence of cells and proangiogenic factors on vascularization of TE skin equivalents, DEDs and developed skin models were assessed using an *ex ovo* CAM assay. The results showed that the mean number of blood vessels were the highest in 2dDR added TE skin equivalents, where the fewest blood vessels were observed in DED groups. The presence of dermal cells and the addition

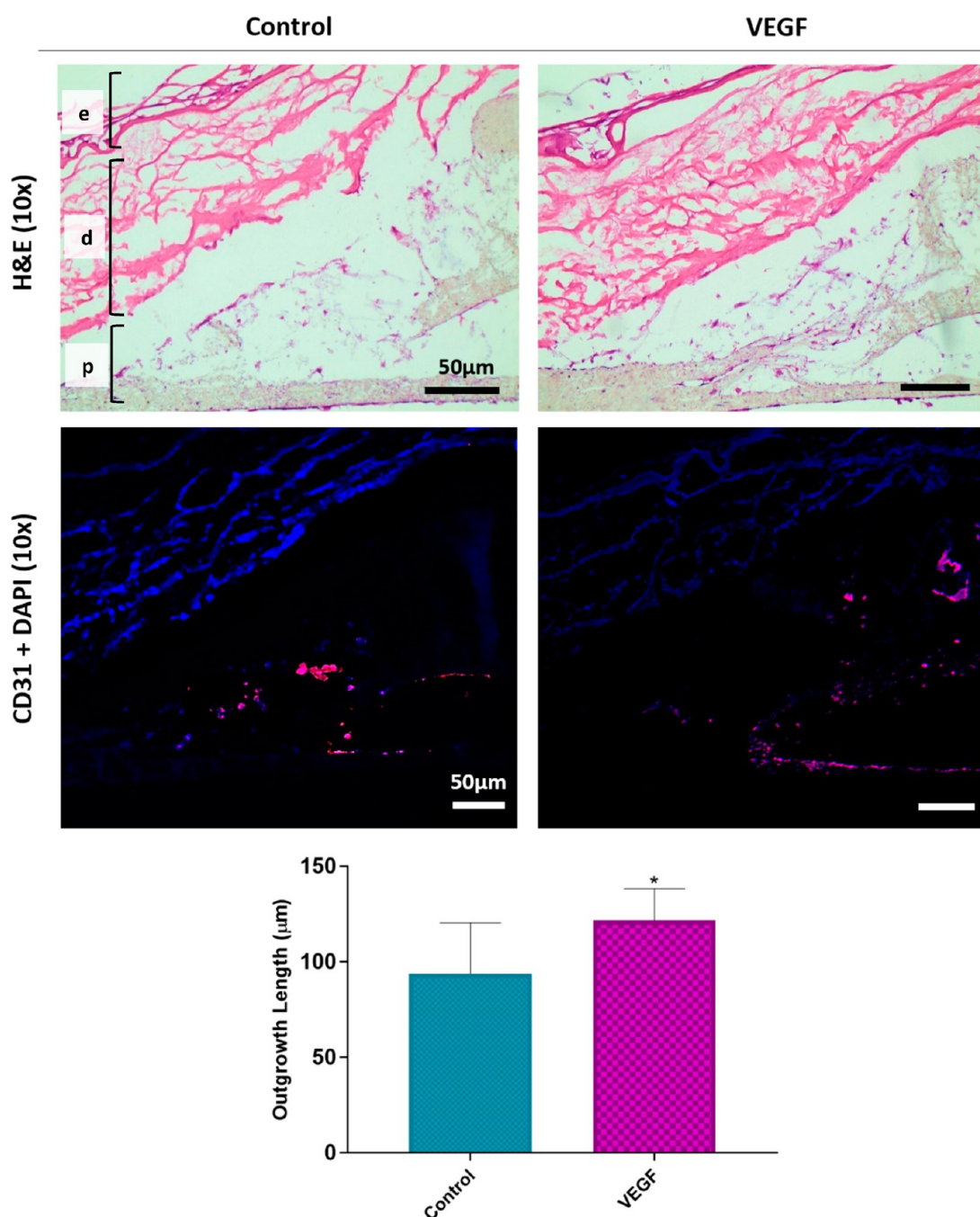


Figure 8. H&E and immunostained (CD31 positive cells are shown with red) sections show that HDMECs were outgrowing from the PHBV channels toward the TE skin models. “e”, “d”, and “p” show epidermis, dermis, and PHBV SVN layers, respectively. The outgrowth was mostly observed from the connection edges of two separate electrospun sheets. Inclusion of VEGF in the growth medium enhanced the outgrowth distance of the HDMECs. The graph shows the quantification of the HDMEC outgrowth distance from PHBV SVN to TE skin models when the growth medium was supplemented with VEGF or nonsupplemented as the control group (* $p \leq 0.05$, $n = 6$).

of both proangiogenic agents significantly increased the mean vessel count growing through the samples (Figure 9).

Mean vessel counts for TE skin models when no proangiogenic agent was added, when administered with 2dDR, and when administered with VEGF were 27.0 ± 1.3 , 34.4 ± 1.9 , and 45.6 ± 2.0 , respectively, whereas the mean vessel count was 19.2 ± 1.5 for the control DED group. None of the implanted groups affected the embryo survival rate, which was over 70% for each group.

Although no complete integration was shown in any of the groups, the DED only group was completely separable from

CAM where TE skin samples either administered with VEGF or 2dDR were better attached to CAMs but without apparent tissue infiltration.

4. DISCUSSION

PHBV is a biocompatible polymer which is widely used in tissue engineering applications,³⁵ and it has previously been reported as a suitable biomaterial to fabricate tissue engineering scaffolds using electrospinning.³⁶ PHBV was chosen for the production of the vascular scaffolds not only due to the previous experiences of our research group^{37–39} but also

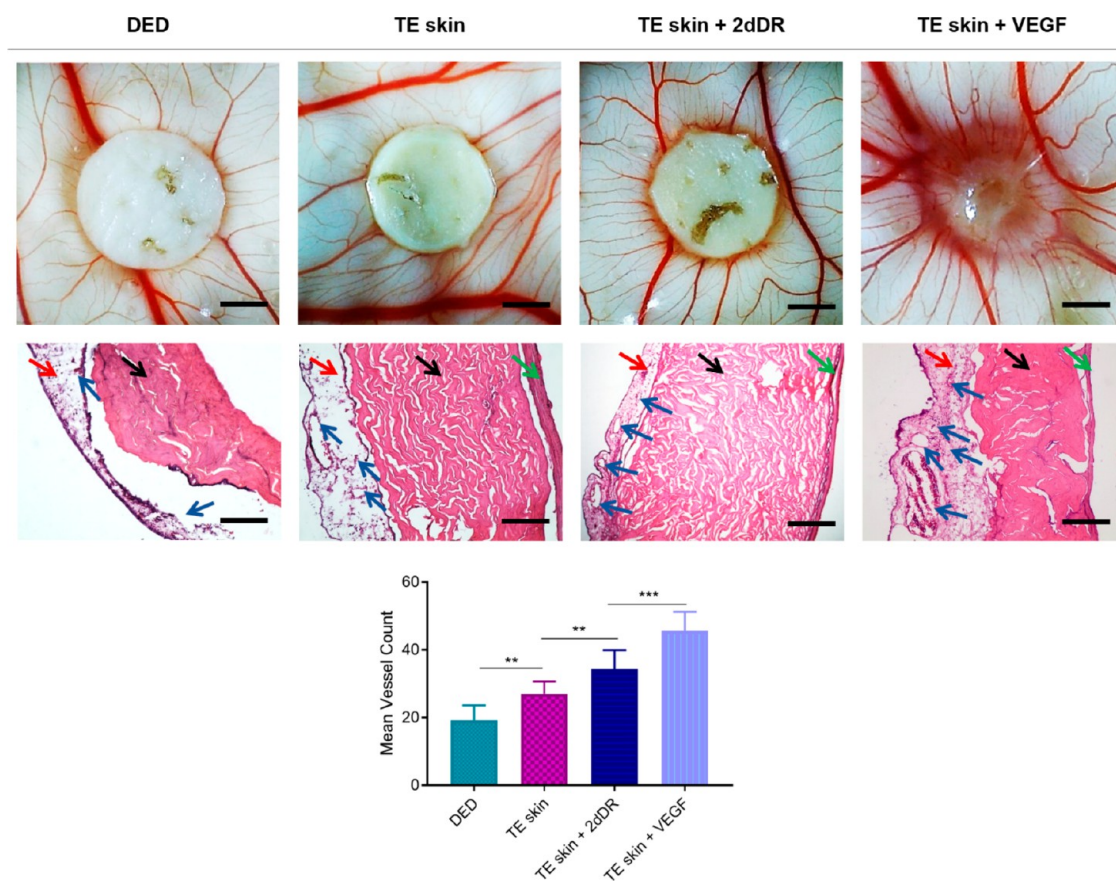


Figure 9. Representative macroimages given in top row show the angiogenic activity of DED, TE skin only, and TE skin with daily addition of 2dDR and VEGF. The histological appearance of the samples can be seen in the middle row. Black, red, green, and blue arrows indicate the CAM, dermal layer, epidermal layer, and blood vessels, respectively. The graph in the bottom row demonstrates the quantification of blood vessels growing toward the samples. Scale bars for macroimages and histological images represents 3 mm and 200 μm , respectively ($***p \leq 0.001$, $**p \leq 0.01$, $n = 4$).

because PHBV has previously been reported as a suitable host for supporting ECs to attach and proliferate on it and form a monolayer.⁴⁰ Both electrospinning and 3D printing techniques have various advantages and are frequently used in tissue engineering applications. The 3D printing technique allows controlling the production of a large number of scaffolds with exactly the same geometries in a short time while electrospinning enables fabricating scaffolds with a wide range of properties in terms of material composition, fiber diameter, thickness, porosity, and degradation rates.^{41–44}

Accordingly, in this work, PHBV nanofibers were successfully manufactured via electrospinning, and alginate, a natural and biocompatible polysaccharide that is largely preferred for biomaterial applications,^{45,46} was used as a sacrificial substrate to create temporary support as interconnected networks. The perfusion of the channels with methylene blue dye showed that the channels were interconnected, and no leakage was observed neither between the two layers of electrospun PHBV nor through the small pores between fibers. The average fiber diameter and pore size were 0.76 ± 0.22 and $2.73 \pm 1.47 \mu\text{m}$, respectively. PHBV fibers in these diameters have been shown to allow transportation of nutrients through fibers while preventing cells from escaping through them for up to 6 weeks.^{38,39} The suture retention test results demonstrated that the PHBV SVN was suitable to be used by suturing the tissue models onto the scaffold. The scaffolds were resistant to suture up to 1.70 and 0.89 MPa pull out strength, respectively, under

dry and wet conditions without any tearing. DuRaine et al. reported the suitability of their TE constructs with a suture retention strength of 1.45 MPa for *in vivo* implantation by suturing them in place.⁴⁷ Selders et al. demonstrated that the suture retention strength of the developed polymer templates was between 0.40 and 1.20 MPa under dry conditions.⁴⁸ Similarly, Syedain et al. showed that acellular vascular grafts with a suture retention of approximately 0.15 MPa (reported as 175 g for a 12.1 mm² graft area) were suitable for suturing *in vivo* as pulmonary artery replacements.⁴⁹

Nanofibers have been shown to provide better surface properties for ECs to adhere and proliferate on them over microfibers.^{50–52} This is likely due to the nanofibers being structurally similar to the ECM of natural tissue with their submicron-scale topography and highly packed morphology.^{50,53} Furthermore, PHBV nanofibers have previously been shown to be a suitable environment for ECs to form an endothelial monolayer.⁴⁰ However, nanofibers also create a physical barrier for cells, which limits the infiltration.⁵⁴ Thus, prior to the outgrowth experiments, holes had to be pierced onto the channels of the scaffolds.

This four-step manufacturing route allowed the production of a large number of identical vascular scaffolds in less than 2 h. Similar fabrication routes of vascular scaffolds combining electrospinning and 3D printing have previously been reported. Jeffries et al. used 3D printed poly(vinyl alcohol) channels as a template in electrospun polydioxanone scaffolds to be used as a

prevascularized implantable construct in future.⁵⁵ Dew et al. previously reported the use of alginate as a sacrificial material in electrospun scaffolds and showed the successful endothelialization of these scaffolds to study the factors that affect neovascularization.^{37,40} However, none of these studies has gone further than studying only one aspect of angiogenesis at the cellular level and did not assess the potential of these scaffolds to be used with biologically relevant tissue models. In this study, we aimed to evaluate the potential use of these bioengineered vascular channels to be used to study angiogenesis *in vitro* and with complex tissue models in comparison with CAM, as a well-vascularized wound bed analogue, for the first time.

The results suggested that it was possible to cellularize the PHBV channels either with HDMECs in isolation or with HDMECs in the presence of HDFs which slightly improved the coverage of the channels with HDMECs as expected from the previously reported studies performed by other groups as well as our group.^{37,56} Although the coverage of the channels was not investigated quantitatively, the qualitative visualization of the cell distribution within the channels showed almost a full coverage of the channels with HDMECs (Figure 5A,B). However, CellTracker-labeled cellularization results showed a more intermittent-like layer within the channel (Figure 5C). The most probable explanation for this is that CellTracker binds target DNA, and it is distributed equally between daughter cells after cell division.⁵⁷ Although it is a very simple and rapid way of identifying different types of cells within a construct, we found that it is not highly effective for estimating the cellular confluency and for investigating the distribution of cells within the channels.

Fibroblasts have previously been reported to play a key role in the angiogenic process by producing considerable amounts of ECM molecules (i.e., collagen, fibronectin, and other molecules), growth and proangiogenic factors which control the shape and density of blood vessels.^{58,59} Although fibroblasts secrete some VEGF, the main role of these cells is to create an ECM in which endothelial cells can be embedded to form tubules. This ECM structure is rich in collagen I and fibronectin.^{60,61} PHBV SVN has been found to provide a suitable environment for HDMECs to form a monolayer either in the presence or absence of HDFs as helper cells. The use of HDFs was found to be desirable depending on the intended use of the PHBV SVN.

For the Matrigel experiments, the PHBV SVN was cellularized with HDMECs in isolation, and the outgrowth of HDMECs was investigated toward the Matrigel. The results showed that HDMECs were outgrowing and forming interconnected tubelike structures within the Matrigel (loaded with either VEGF or 2dDR) close to edges of the pierced synthetic PHBV channels. The tubelike formed structures were more obvious and well-organized in the VEGF loaded Matrigel group when compared with 2dDR loaded and control groups. VEGF is an effective and well-established proangiogenic factor⁶² which has been proven to be a regulator of EC proliferation, migration, and survival.^{63,64} 2dDR, a small sugar that naturally occurs in the body as a result of the enzymatic degradation of thymidine to thymine,⁶⁵ has recently been reported to have potential to induce angiogenesis *in vitro*,³⁰ in *ex ovo* CAM assay,²⁵ and in diabetic rats.⁶⁶

The formation of the tubelike structures was pretty similar to those which can be observed in Matrigel tube formation assays. *In vivo*, endothelial cells are in direct contact with a basement

membrane which is specific and biologically functional for enabling endothelial cells to form tube structures.⁶⁷ This biologically active protein mixture is a wonderful candidate for mimicking the native basement membrane of endothelial cells *in vitro* and promotes endothelial cells to form tubelike capillary structures.⁶⁸ Kubota et al. seeded endothelial cells on a mimicked basement membrane and reported that endothelial cells could attach and form tubelike capillary structures within 2–3 h.⁶⁹ Our observations were in line with the literature where VEGF has been reported to regulate outgrowth of ECs.^{70–72} Loading of 2dDR into Matrigel also stimulated ECs to form tubelike structures as we have previously reported the promotion of tube formation in Matrigel assay.³⁰ The proposed platform can be used to study more than one aspect of angiogenesis *in vitro* when combined with Matrigel. However, several factors should be considered while using the developed model for the study of angiogenesis:

- (i) Matrigel is a protein gel mixture which is rich in ECM proteins such as laminin, collagen heparin sulfate, proteoglycans, etc. However, the exact concentrations of the ingredients are not clearly defined, and it shows high batch-to-batch variations.⁷³
- (ii) The thickness of Matrigel should be considered as the thickness of gels has previously been shown to have a negative impact on the survival of ECs and HDFs.⁷⁴
- (iii) HDMECs are very sensitive to culture conditions and show batch-to-batch variations.⁷⁵ These variations of ECs have been previously shown to be a cause for not being reproducible for *in vitro* angiogenesis models.⁷⁶
- (iv) The holes pierced on SVN channels were randomly oriented, and their positions and diameters might have an impact on the variations in the outgrowth of HDMECs.

Following the Matrigel experiments, a more physiologically relevant tissue model, the TE skin model, was used with PHBV SVN to study vascularization of a reconstructed human skin model. The TE skin model was successfully developed using a well-established protocol.²⁸ The air–liquid interface has previously been confirmed to provide a stimulus for the gradual differentiation of keratinocytes.²³ The histological evaluation of the reconstructed TE skin models showed that the developed TE skin model achieved a normal-looking gross skin morphology in 14 days. A multilayered epithelium was formed and found to be well attached to the dermis. Following the reconstruction of TE skin, after 7 day culture at the air–liquid interface, the TE skin equivalent was attached to the top surface of the PHBV SVN and cultured for further 7 days at the air–liquid interface.

The outgrowth of HDMECs toward the TE skin model was mostly observed from the connection edges of two separate electrospun sheets, and the inclusion of VEGF to the growth media significantly increased the outgrowth distance of HDMECs approximately 4.4-fold when compared to controls. However, cells were not found to be invading into the dermal layer of the developed skin models either supplemented with VEGF or not. Santos et al., previously demonstrated that starch-based scaffolds combined with growth factors and fibrin sealant (fibrinogen 75–115 mg/mL, thrombin 4 IU/mL) were capable of promoting vascular infiltration to newly formed tissue *in vivo*.⁷⁷ In addition, the concentration of fibrin glue used in this study is also approximately 3–4 times lower than some commercially available skin graft sealant fibrin glues.^{78,79}

We have previously demonstrated that fibrin glue with a fibrinogen concentration of 18.75 mg/mL, a similarly high concentration as used in this study, did not hinder cell outgrowth from tissue explants.⁸⁰ Thus, the concentration of fibrin glue does not seem to be the major cause of the prevention of cell penetration. The most probable explanations for this are that the outgrowth direction of HDMECs was against gravity; the rate of outgrowth of HDMECs from PHBV channels was low. Furthermore, the orientations, positions, and diameters of the manually pierced random holes might also have negatively affected the outgrowth of HDMECs. Our group had previously explored the endothelialization of a TE skin model and reported that the cells struggled to enter the TE skin and showed no signs of being organized when they did enter.²⁴

CAM is a well-vascularized membrane, and we hypothesized that CAM might represent a very well-vascularized wound bed. Thus, as a positive control experiment, we implanted the TE skin models to assess the vascularization of reconstructed skin models from CAM. The results of the *ex ovo* CAM assay were in compliance with the results obtained from PHBV SVN studies. Although CAM is a highly vascularized and dynamic environment with fast proliferating embryonic cells,⁸¹ the results showed that there was no sign of blood vessel or tissue integration into the dermal layer of the reconstructed skin substitutes. However, the presence of dermal cells (fibroblasts and keratinocytes) significantly improved the vascularization in the area of implantation (toward the implanted TE skin) in comparison with DED (with no cells). In addition, the administration of VEGF and 2dDR showed a further increase in angiogenic activity. Although the major function of fibroblasts is to synthesize and maintain ECM structure, they have been reported to produce collagen, fibronectin, proteoglycans, and connective growth factors, especially in response to wounding.^{82,83} They have also been reported as producing soluble angiogenic growth factors such as VEGF,⁸⁴ transforming growth factor-beta (TGF- β),⁸⁵ and platelet-derived growth factor (PDGF).⁸⁶ Furthermore, keratinocytes have previously been reported to improve the proliferation of endothelial cells and to express VEGF.⁸⁷ Recently, the presence of cells and *in vitro* generated ECM has also been shown to improve angiogenesis in the *ex ovo* CAM assay.^{88,89} The enhanced angiogenic properties of TE skin over DED on CAM might be validated by the studies given above.

While an increased angiogenic activity was observed when cells and drugs were presented to CAMs, the histological evaluation of the implanted TE skin models showed that there was no tissue infiltration and vascularization through the dermal layer of the reconstructed TE skin models. Although no vascularization was observed in any of the implants, one important thing to note was that the inclusion of dermal cells (fibroblasts and keratinocytes) and proangiogenic agents (VEGF and 2dDR) improved the “take” of the TE skin model by CAM when compared to DED with no cells. The attachment of the TE skin model to CAM (either supplemented with proangiogenic agents or not) was stronger whereas the DED showed no integration with CAM, and it was easily separable from the surface of the membrane after the implantation period.

The developed platform showed encouraging results to be used as an *in vitro* platform to study angiogenesis at either cellular or tissue levels. Future studies need to be conducted to improve the reliability of the proposed *in vitro* platform and to

standardize the methodology for seeding of the cells, loading of Matrigel to the synthetic vascular scaffolds, piercing holes, and assessing the angiogenesis. In the scope of this study, only one tissue model was developed and assessed on PHBV SVN. However, promising results have shown that, through further improvements, the PHBV SVN can offer a great platform for studying *in vitro* vascularization of tissue models.

5. CONCLUSION

Herein, we demonstrated the development of a polymeric vascular network to be used as an *in vitro* platform to study angiogenesis and to investigate the vascularization of complex tissue models. The nanofibrous channels have been found to provide a suitable environment for HDMECs to form a monolayer in either the presence or absence of HDFs. The indirect coculture with HDFs has been shown to be a desirable approach depending on the intended use of the PHBV SVN. The developed *in vitro* platform enabled the study of more than one aspect of angiogenesis (migration and tube formation) when combined with Matrigel. In addition, PHBV SVN provided a convenient platform to study vascularization of a reconstructed human skin model as a physiologically more relevant and complex structure. All of these results demonstrated that the developed PHBV SVN could offer a really good platform to study angiogenesis *in vitro* with potential developments.

■ AUTHOR INFORMATION

Corresponding Author

Sheila MacNeil – Department of Materials Science and Engineering, Krotto Research Institute, University of Sheffield, Sheffield S3 7HQ, United Kingdom; Email: s.macneil@sheffield.ac.uk

Authors

Serkan Dikici – Department of Materials Science and Engineering, Krotto Research Institute, University of Sheffield, Sheffield S3 7HQ, United Kingdom; orcid.org/0000-0001-9933-5254

Frederik Claeysens – Department of Materials Science and Engineering, Krotto Research Institute, University of Sheffield, Sheffield S3 7HQ, United Kingdom; orcid.org/0000-0002-1030-939X

Complete contact information is available at:
<https://pubs.acs.org/10.1021/acsbomaterials.0c00191>

Notes

The authors declare no competing financial interest.
Ethical Statement: Ethical approval for the tissue acquisition was granted by the National Research Ethics Service (NRES) Committee Yorkshire and The Humber–Sheffield (REC ref., 15/YH/0177; REC opinion date, 03/06/2015). The authors state that they have obtained appropriate institutional review board approval or have followed the principles outlined in the Declaration of Helsinki for all human or animal experimental investigations. All CAM assay experiments were carried out according to Home Office, UK guidelines.

■ ACKNOWLEDGMENTS

The authors are grateful to the Turkish Ministry of National Education for the funding of the PhD award to Serkan Dikici. They also acknowledge the Engineering and Physical Sciences

Research Council (Grant EP/I007695/1) and the Medical Research Council (Grant MR/L012669/1) for funding the equipment used in this study. We thank Dr. Anthony Bullock for his guidance on the reconstruction of the human skin model.

REFERENCES

- (1) Risau, W. Mechanisms of Angiogenesis. *Nature* **1997**, *386* (6626), 671–674.
- (2) Novosel, E. C.; Kleinhans, C.; Kluger, P. J. Vascularization Is the Key Challenge in Tissue Engineering. *Adv. Drug Delivery Rev.* **2011**, *63* (4), 300–311.
- (3) Stryker, Z. L.; Rajabi, M.; Davis, P. J.; Mousa, S. A. Evaluation of Angiogenesis Assays. *Biomedicines* **2019**, *7* (2), 37.
- (4) Staton, C. A.; Stribbling, S. M.; Tazzyman, S.; Hughes, R.; Brown, N. J.; Lewis, C. E. Current Methods for Assaying Angiogenesis in Vitro and in Vivo. *Int. J. Exp. Pathol.* **2004**, *85* (5), 233–248.
- (5) Ravi, M.; Paramesh, V.; Kaviya, S. R.; Anuradha, E.; Paul Solomon, F. D. 3D Cell Culture Systems: Advantages and Applications. *J. Cell. Physiol.* **2015**, *230* (1), 16–26.
- (6) Wang, X. Y.; Jin, Z. H.; Gan, B. W.; Lv, S. W.; Xie, M.; Huang, W. H. Engineering Interconnected 3D Vascular Networks in Hydrogels Using Molded Sodium Alginate Lattice as the Sacrificial Template. *Lab Chip* **2014**, *14* (15), 2709–2716.
- (7) Li, S.; Liu, Y. Y.; Liu, L. J.; Hu, Q. X. A Versatile Method for Fabricating Tissue Engineering Scaffolds with a Three-Dimensional Channel for Prevasculature Networks. *ACS Appl. Mater. Interfaces* **2016**, *8* (38), 25096–25103.
- (8) Miller, J. S.; Stevens, K. R.; Yang, M. T.; Baker, B. M.; Nguyen, D. H. T.; Cohen, D. M.; Toro, E.; Chen, A. A.; Galie, P. A.; Yu, X.; et al. Rapid Casting of Patterned Vascular Networks for Perfusible Engineered Three-Dimensional Tissues. *Nat. Mater.* **2012**, *11* (9), 768–774.
- (9) Kim, G. H.; Son, J. G.; Park, S.; Kim, W. D. Hybrid Process for Fabricating 3D Hierarchical Scaffolds Combining Rapid Prototyping and Electrospinning. *Macromol. Rapid Commun.* **2008**, *29* (19), 1577–1581.
- (10) Ortega, I.; Dew, L.; Kelly, A. G.; Chong, C. K.; Macneil, S.; Claeysens, F. Fabrication of Biodegradable Synthetic Perfusible Vascular Networks via a Combination of Electrospinning and Robocasting. *Biomater. Sci.* **2015**, *3* (4), 592–596.
- (11) Chwalek, K.; Bray, L. J.; Werner, C. Tissue-Engineered 3D Tumor Angiogenesis Models: Potential Technologies for Anti-Cancer Drug Discovery. *Adv. Drug Delivery Rev.* **2014**, *79*, 30–39.
- (12) MacNeil, S. Progress and Opportunities for Tissue-Engineered Skin. *Nature* **2007**, *445*, 874–880.
- (13) Chau, D. Y.; Johnson, C.; Macneil, S.; Haycock, J. W.; Ghaemmaghami, A. M. The Development of a 3D Immunocompetent Model of Human Skin. *Biofabrication* **2013**, *5* (3), 35011.
- (14) Groeber, F.; Holeiter, M.; Hampel, M.; Hinderer, S.; Schenke-Layland, K. Skin Tissue Engineering - In Vivo and in Vitro Applications. *Adv. Drug Delivery Rev.* **2011**, *63*, 352–366.
- (15) Facy, V.; Flouret, V.; Régnier, M.; Schmidt, R. Reactivity of Langerhans Cells in Human Reconstructed Epidermis to Known Allergens and UV Radiation. *Toxicol. In Vitro* **2005**, *19* (6), 787–795.
- (16) Kandárová, H.; Liebsch, M.; Schmidt, E.; Genschow, E.; Traue, D.; Spielmann, H.; Meyer, K.; Steinhoff, C.; Tornier, C.; De Wever, B.; et al. Assessment of the Skin Irritation Potential of Chemicals by Using the Skin Ethic Reconstructed Human Epidermal Model and the Common Skin Irritation Protocol Evaluated in the ECVAM Skin Irritation Validation Study. *ATLA, Altern. Lab. Anim.* **2006**, *34* (4), 393–406.
- (17) Bessou, S.; Surlève-Bazeille, J. E.; Pain, C.; Donatien, P.; Taïeb, A. Ex Vivo Study of Skin Phototypes. *J. Invest. Dermatol.* **1996**, *107* (5), 684–688.
- (18) Meier, F.; Nesbit, M.; Hsu, M.-Y.; Martin, B.; Van Belle, P.; Elder, D. E.; Schaumburg-Lever, G.; Garbe, C.; Walz, T. M.; Donatien, P.; et al. Human Melanoma Progression in Skin Reconstructs. *Am. J. Pathol.* **2000**, *156* (1), 193–200.
- (19) Admane, P.; Gupta, A. C.; Jois, P.; Roy, S.; Chandrasekharan Lakshmanan, C.; Kalsi, G.; Bandyopadhyay, B.; Ghosh, S. Direct 3D Bioprinted Full-Thickness Skin Constructs Recapitulate Regulatory Signaling Pathways and Physiology of Human Skin. *Bioprinting* **2019**, *15*, No. e00051.
- (20) Kim, B. S.; Gao, G.; Kim, J. Y.; Cho, D. W. 3D Cell Printing of Perfusible Vascularized Human Skin Equivalent Composed of Epidermis, Dermis, and Hypodermis for Better Structural Recapitulation of Native Skin. *Adv. Healthcare Mater.* **2019**, *8* (7), 1801019.
- (21) Kolesky, D. B.; Homan, K. A.; Skylar-Scott, M. A.; Lewis, J. A. Three-Dimensional Bioprinting of Thick Vascularized Tissues. *Proc. Natl. Acad. Sci. U. S. A.* **2016**, *113* (12), 3179–3184.
- (22) John, S.; Kesting, M. R.; Paulitschke, P.; Stöckelhuber, M.; von Bomhard, A. Development of a Tissue-Engineered Skin Substitute on a Base of Human Amniotic Membrane. *J. Tissue Eng.* **2019**, *10*, 1–14.
- (23) MacNeil, S.; Shepherd, J.; Smith, L. Production of Tissue-Engineered Skin and Oral Mucosa for Clinical and Experimental Use. *Methods Mol. Biol.* **2011**, *695*, 129–153.
- (24) Sahota, P. S.; Burn, J. L.; Heaton, M.; Freedlander, E.; Suvarna, S. K.; Brown, N. J.; Mac Neil, S. Development of a Reconstructed Human Skin Model for Angiogenesis. *Wound Repair Regen.* **2003**, *11* (4), 275–284.
- (25) Dikici, S.; Mangir, N.; Claeysens, F.; Yar, M.; MacNeil, S. Exploration of 2-Deoxy-D-Ribose and 17 β -Estradiol as Alternatives to Exogenous VEGF to Promote Angiogenesis in Tissue-Engineered Constructs. *Regener. Med.* **2019**, *14* (3), 179–197.
- (26) Aldemir Dikici, B.; Sherborne, C.; Reilly, G. C.; Claeysens, F. Emulsion Templated Scaffolds Manufactured from Photocurable Polycaprolactone. *Polymer* **2019**, *175*, 243–254.
- (27) Aldemir Dikici, B.; Dikici, S.; Reilly, G. C.; MacNeil, S.; Claeysens, F. A Novel Bilayer Polycaprolactone Membrane for Guided Bone Regeneration: Combining Electrospinning and Emulsion Templating. *Materials* **2019**, *12* (16), 2643.
- (28) Ghosh, M. M.; Boyce, S.; Layton, C.; Freedlander, E.; Mac Neil, S. A Comparison of Methodologies for the Preparation of Human Epidermal-Dermal Composites. *Ann. Plast. Surg.* **1997**, *39*, 390–404.
- (29) Chakrabarty, K. H.; Dawson, R. A.; Harris, P.; Layton, C.; Babu, M.; Gould, L.; Phillips, J.; Leigh, I.; Green, C.; Freedlander, E.; et al. Development of Autologous Human Dermal-Epidermal Composites Based on Sterilized Human Allodermis for Clinical Use. *Br. J. Dermatol.* **1999**, *141* (5), 811–823.
- (30) Dikici, S.; Aldemir Dikici, B.; Bhaloo, S. I.; Balcells, M.; Edelman, E. R.; Macneil, S.; Reilly, G. C.; Sherborne, C.; Claeysens, F. Assessment of the Angiogenic Potential of 2-Deoxy-D-Ribose Using a Novel in Vitro 3D Dynamic Model in Comparison with Established in Vitro Assays. *Front. Bioeng. Biotechnol.* **2020**, *7*, 451.
- (31) DeCicco-Skinner, K. L.; Henry, G. H.; Cataisson, C.; Tabib, T.; Curtis Gwilliam, J.; Watson, N. J.; Bullwinkle, E. M.; Falkenburg, L.; O'Neill, R. C.; Morin, A.; et al. Endothelial Cell Tube Formation Assay for the in Vitro Study of Angiogenesis. *J. Visualized Exp.* **2014**, No. 91, No. e51312.
- (32) Brown, R. M.; Meah, C. J.; Heath, V. L.; Styles, I. B.; Bicknell, R. Tube-Forming Assays. *Methods Mol. Biol.* **2016**, *1430*, 149–157.
- (33) Currie, L. J.; Sharpe, J. R.; Martin, R. The Use of Fibrin Glue in Skin Grafts and Tissue-Engineered Skin Replacements: A Review. *Plastic and Reconstructive Surgery* **2001**, *108*, 1713.
- (34) Mangir, N.; Dikici, S.; Claeysens, F.; Macneil, S. Using Ex Ovo Chick Chorioallantoic Membrane (CAM) Assay to Evaluate the Biocompatibility and Angiogenic Response to Biomaterials. *ACS Biomater. Sci. Eng.* **2019**, *5* (7), 3190–3200.
- (35) Wang, L.; Du, J.; Cao, D.; Wang, Y. Recent Advances and the Application of Poly(3-Hydroxybutyrate-Co-3-Hydroxyvalerate) as Tissue Engineering Materials. *J. Macromol. Sci., Part A: Pure Appl. Chem.* **2013**, *50* (8), 885–893.

- (36) Alagoz, A. S.; Rodriguez-Cabello, J. C.; Hasirci, V. PHBV Wet-Spun Scaffold Coated with ELR-REDV Improves Vascularization for Bone Tissue Engineering. *Biomed. Mater.* **2018**, *13* (5), 055010.
- (37) Ortega, I.; Dew, L.; Kelly, A. G.; Chong, C. K.; Macneil, S.; Claeysens, F. Fabrication of Biodegradable Synthetic Perfusible Vascular Networks via a Combination of Electrospinning and Robocasting. *Biomater. Sci.* **2015**, *3* (4), 592–596.
- (38) Bye, F. J.; Bullock, A. J.; Singh, R.; Sefat, F.; Roman, S.; MacNeil, S. Development of a Basement Membrane Substitute Incorporated Into an Electrospun Scaffold for 3D Skin Tissue Engineering. *J. Biomater. Tissue Eng.* **2014**, *4* (9), 686–692.
- (39) Bye, F. J.; Bissoli, J.; Black, L.; Bullock, A. J.; Puwanun, S.; Moharamzadeh, K.; Reilly, G. C.; Ryan, A. J.; MacNeil, S. Development of Bilayer and Trilayer Nanofibrous/Microfibrous Scaffolds for Regenerative Medicine. *Biomater. Sci.* **2013**, *1* (9), 942–951.
- (40) Dew, L.; English, W. R.; Ortega, I.; Claeysens, F.; Macneil, S. Fabrication of Biodegradable Synthetic Vascular Networks and Their Use as a Model of Angiogenesis. *Cells Tissues Organs* **2016**, *202* (5–6), 319–328.
- (41) Lannutti, J.; Reneker, D.; Ma, T.; Tomasko, D.; Farson, D. Electrospinning for Tissue Engineering Scaffolds. *Mater. Sci. Eng., C* **2007**, *27* (3), 504–509.
- (42) Blackwood, K. A.; McKean, R.; Canton, I.; Freeman, C. O.; Franklin, K. L.; Cole, D.; Brook, I.; Farthing, P.; Rimmer, S.; Haycock, J. W.; et al. Development of Biodegradable Electrospun Scaffolds for Dermal Replacement. *Biomaterials* **2008**, *29* (21), 3091–3104.
- (43) Szentivanyi, A.; Chakradeo, T.; Zernetsch, H.; Glasmacher, B. Electrospun Cellular Microenvironments: Understanding Controlled Release and Scaffold Structure. *Adv. Drug Delivery Rev.* **2011**, *63* (4), 209–220.
- (44) Pham, Q. P.; Sharma, U.; Mikos, A. G. Electrospinning of Polymeric Nanofibers for Tissue Engineering Applications: A Review. *Tissue Eng.* **2006**, *12* (5), 1197–1211.
- (45) Augst, A. D.; Kong, H. J.; Mooney, D. J. Alginate Hydrogels as Biomaterials. *Macromol. Biosci.* **2006**, *6* (8), 623–633.
- (46) Rowley, J. A.; Madlambayan, G.; Mooney, D. J. Alginate Hydrogels as Synthetic Extracellular Matrix Materials. *Biomaterials* **1999**, *20* (1), 45–53.
- (47) DuRaine, G. D.; Arzi, B.; Lee, J. K.; Lee, C. A.; Responde, D. J.; Hu, J. C.; Athanasiou, K. A. Biomechanical Evaluation of Suture-Holding Properties of Native and Tissue-Engineered Articular Cartilage. *Biomech. Model. Mechanobiol.* **2015**, *14* (1), 73–81.
- (48) Selders, G. S.; Fetz, A. E.; Speer, S. L.; Bowlin, G. L. Fabrication and Characterization of Air-Impedance Electrospun Polydioxanone Templates. *Electrospinning* **2015**, *1* (1), 20–30.
- (49) Syedain, Z.; Reimer, J.; Lahti, M.; Berry, J.; Johnson, S.; Tranquillo, R. T. Tissue Engineering of Acellular Vascular Grafts Capable of Somatic Growth in Young Lambs. *Nat. Commun.* **2016**, *7*, 12951.
- (50) Keun Kwon, I.; Kidoaki, S.; Matsuda, T. Electrospun Nano- to Microfiber Fabrics Made of Biodegradable Copolyesters: Structural Characteristics, Mechanical Properties and Cell Adhesion Potential. *Biomaterials* **2005**, *26* (18), 3929–3939.
- (51) Beachley, V.; Wen, X. Polymer Nanofibrous Structures: Fabrication, Biofunctionalization, and Cell Interactions. *Prog. Polym. Sci.* **2010**, *35* (7), 868–892.
- (52) Venugopal, J.; Low, S.; Choon, A. T.; Ramakrishna, S. Interaction of Cells and Nanofiber Scaffolds in Tissue Engineering. *J. Biomed. Mater. Res., Part B* **2008**, *84* (1), 34–48.
- (53) Gunn, J.; Zhang, M. Polyblend Nanofibers for Biomedical Applications: Perspectives and Challenges. *Trends Biotechnol.* **2010**, *28* (4), 189–197.
- (54) Shafei, S.; Foroughi, J.; Chen, Z.; Wong, C. S.; Naebe, M. Short Oxygen Plasma Treatment Leading to Long-Term Hydrophilicity of Conductive PCL-PPy Nanofiber Scaffolds. *Polymers (Basel, Switz.)* **2017**, *9* (11), 614.
- (55) Jeffries, E. M.; Nakamura, S.; Lee, K. W.; Clampffer, J.; Ijima, H.; Wang, Y. Micropatterning Electrospun Scaffolds to Create Intrinsic Vascular Networks. *Macromol. Biosci.* **2014**, *14* (11), 1514–1520.
- (56) Dew, L. *Development of Angiogenic Models to Investigate Neovascularisation for Tissue Engineering Applications*. PhD Thesis, The University of Sheffield, 2015.
- (57) Zhou, W.; Kang, H. C.; O’Grady, M.; Chambers, K. M.; Dubbels, B.; Melquist, P.; Gee, K. R. Cell Trace™ Far Red & CellTracker™ Deep Red—Long Term Live Cell Tracking for Flow Cytometry and Fluorescence Microscopy. *J. Biol. Methods* **2016**, *3* (1), No. e38.
- (58) Black, A. F.; Berthod, F.; L’heureux, N.; Germain, L.; Auger, F. A. In Vitro Reconstruction of a Human Capillary-like Network in a Tissue-Engineered Skin Equivalent. *FASEB J.* **1998**, *12* (1), 1331–1340.
- (59) Hudon, V.; Berthod, F.; Black, A. F.; Damour, O.; Germain, L.; Auger, F. A. A Tissue-Engineered Endothelialized Dermis to Study the Modulation of Angiogenic and Angiostatic Molecules on Capillary-like Tube Formation in Vitro. *Br. J. Dermatol.* **2003**, *148* (6), 1094–1104.
- (60) Sorrell, J. M.; Baber, M. A.; Caplan, A. I. A Self-Assembled Fibroblast-Endothelial Cell Co-Culture System That Supports in Vitro Vasculogenesis by Both Human Umbilical Vein Endothelial Cells and Human Dermal Microvascular Endothelial Cells. *Cells Tissues Organs* **2007**, *186* (3), 157–168.
- (61) Bishop, E. T.; Bell, G. T.; Bloor, S.; Broom, I. J.; Hendry, N. F.; Wheatley, D. N. An in Vitro Model of Angiogenesis: Basic Features. *Angiogenesis* **1999**, *3*, 335–344.
- (62) Hoeben, A. N. N.; Landuyt, B.; Highley, M. S. M.; Wildiers, H.; Van Oosterom, A. T.; De Bruijn, E. A. Vascular Endothelial Growth Factor and Angiogenesis. *Pharmacol. Rev.* **2004**, *56* (4), 549–580.
- (63) Olsson, A. K.; Dimberg, A.; Kreuger, J.; Claesson-Welsh, L. VEGF Receptor Signalling - In Control of Vascular Function. *Nat. Rev. Mol. Cell Biol.* **2006**, *7* (5), 359–371.
- (64) Wang, S.; Li, X.; Parra, M.; Verdin, E.; Bassel-Duby, R.; Olson, E. N. Control of Endothelial Cell Proliferation and Migration by VEGF Signaling to Histone Deacetylase 7. *Proc. Natl. Acad. Sci. U. S. A.* **2008**, *105* (22), 7738–7743.
- (65) Brown, N. S.; Bicknell, R. Thymidine Phosphorylase, 2-Deoxy-D-Ribose and Angiogenesis. *Biochem. J.* **1998**, *334*, 1–8.
- (66) Azam, M.; Dikici, S.; Roman, S.; Mehmood, A.; Chaudhry, A. A.; U Rehman, I.; MacNeil, S.; Yar, M. Addition of 2-Deoxy-d-Ribose to Clinically Used Alginate Dressings Stimulates Angiogenesis and Accelerates Wound Healing in Diabetic Rats. *J. Biomater. Appl.* **2019**, *34* (4), 463–475.
- (67) Kalluri, R. Basement Membranes: Structure, Assembly and Role in Tumour Angiogenesis. *Nat. Rev. Cancer* **2003**, *3* (6), 422–433.
- (68) Kleinman, H. K.; Martin, G. R. Matrigel: Basement Membrane Matrix with Biological Activity. *Semin. Cancer Biol.* **2005**, *15* (5), 378–386.
- (69) Kubota, Y.; Kleinman, H. K.; Martin, G. R.; Lawley, T. J. Role of Laminin and Basement Membrane in the Morphological Differentiation of Human Endothelial Cells into Capillary-like Structures. *J. Cell Biol.* **1988**, *107* (4), 1589–1598.
- (70) Blanco, R.; Gerhardt, H. VEGF and Notch in Tip and Stalk Cell Selection. *Cold Spring Harbor Perspect. Med.* **2013**, *3* (1), 657–659.
- (71) Gerhardt, H.; Golding, M.; Fruttiger, M.; Ruhrberg, C.; Lundkvist, A.; Abramsson, A.; Jeltsch, M.; Mitchell, C.; Alitalo, K.; Shima, D.; et al. VEGF Guides Angiogenic Sprouting Utilizing Endothelial Tip Cell Filopodia. *J. Cell Biol.* **2003**, *161* (6), 1163–1177.
- (72) Jakobsson, L.; Franco, C. A.; Bentley, K.; Collins, R. T.; Ponsoen, B.; Aspalter, I. M.; Rosewell, I.; Busse, M.; Thurston, G.; Medvinsky, A.; et al. Endothelial Cells Dynamically Compete for the Tip Cell Position during Angiogenic Sprouting. *Nat. Cell Biol.* **2010**, *12* (10), 943–953.
- (73) Reis, L.; Chiu, L. L. Y.; Feric, N.; Fu, L.; Radisic, M. Injectable Biomaterials for Cardiac Regeneration and Repair. *In Cardiac*

Regeneration and Repair: Biomaterials and Tissue Engineering **2014**, 49–81.

(74) Staton, C. A.; Reed, M. W. R.; Brown, N. J. A Critical Analysis of Current in Vitro and in Vivo Angiogenesis Assays. *Int. J. Exp. Pathol.* **2009**, *90* (3), 195–221.

(75) Richard, L.; Velasco, P.; Detmar, M. Isolation and Culture of Microvascular Endothelial Cells. *Methods Mol. Med.* **1998**, *18*, 261–269.

(76) Bahramsoltani, M.; Harms, T.; Drewes, B.; Plendl, J. Searching for Markers to Identify Angiogenic Endothelial Cells: A Proteomic Approach. *Clin. Hemorheol. Microcirc.* **2013**, *55* (2), 255–269.

(77) Santos, T. C.; Morton, T. J.; Moritz, M.; Pfeifer, S.; Reise, K.; Marques, A. P.; Castro, A. G.; Reis, R. L.; Van Griensven, M. Vascular Endothelial Growth Factor and Fibroblast Growth Factor-2 Incorporation in Starch-Based Bone Tissue-Engineered Constructs Promote the in Vivo Expression of Neovascularization Mediators. *Tissue Eng., Part A* **2013**, *19* (7–8), 834–848.

(78) Reddy, K. S.; Chittoria, R. K.; Babu, P.; Marimuthu, S. K.; Kumar, S. H.; Subbarayan, E. K.; Chavan, V.; Mohapatra, D. P.; Sivakumar, D. K.; Friji, M. T. Effectiveness of Fibrin Glue in Adherence of Skin Graft. *J. Cutan. Aesthet. Surg.* **2017**, *10* (2), 72–75.

(79) Park, W.; Kim, W. H.; Lee, C. H.; Kim, D. Y.; Choi, J. H.; Huh, J. W.; Sung, H. M.; Kim, I. S.; Kweon, O. K. Comparison of Two Fibrin Glues in Anastomoses and Skin Closure. *J. Vet. Med., A* **2002**, *49* (7), 385–389.

(80) Deshpande, P.; Ramachandran, C.; Sefat, F.; Mariappan, I.; Johnson, C.; McKean, R.; Hannah, M.; Sangwan, V. S.; Claeysens, F.; Ryan, A. J.; et al. Simplifying Corneal Surface Regeneration Using a Biodegradable Synthetic Membrane and Limbal Tissue Explants. *Biomaterials* **2013**, *34* (21), 5088–5106.

(81) Gabrielli, M. G.; Accili, D. The Chick Chorioallantoic Membrane: A Model of Molecular, Structural, and Functional Adaptation to Transepithelial Ion Transport and Barrier Function during Embryonic Development. *J. Biomed. Biotechnol.* **2010**, *2010*, 940741.

(82) Sato, N.; Maehara, N.; Goggins, M. Gene Expression Profiling of Tumor-Stromal Interactions between Pancreatic Cancer Cells and Stromal Fibroblasts. *Cancer Res.* **2004**, *64* (19), 6950–6956.

(83) Chang, H. Y.; Sneddon, J. B.; Alizadeh, A. A.; Sood, R.; West, R. B.; Montgomery, K.; Chi, J. T.; Van De Rijn, M.; Botstein, D.; Brown, P. O. Gene Expression Signature of Fibroblast Serum Response Predicts Human Cancer Progression: Similarities between Tumors and Wounds. *PLoS Biol.* **2004**, *2* (2), e7.

(84) Kellouche, S.; Mourah, S.; Bonnefoy, A.; Schoëvaert, D.; Podgorniak, M. P.; Calvo, F.; Hoylaerts, M. F.; Legrand, C.; Dosquet, C. Platelets, Thrombospondin-1 and Human Dermal Fibroblasts Cooperate for Stimulation of Endothelial Cell Tubulogenesis through VEGF and PAI-1 Regulation. *Exp. Cell Res.* **2007**, *313* (3), 486–499.

(85) Paunescu, V.; Bojin, F. M.; Tatu, C. A.; Gavriluc, O. I.; Rosca, A.; Gruia, A. T.; Tanasie, G.; Bunu, C.; Crisnic, D.; Gherghiceanu, M.; et al. Tumour-Associated Fibroblasts and Mesenchymal Stem Cells: More Similarities than Differences. *J. Cell. Mol. Med.* **2011**, *15* (3), 635–646.

(86) Antoniades, H. N.; Galanopoulos, T.; Neville-Golden, J.; Kiritsy, C. P.; Lynch, S. E. Injury Induces in Vivo Expression of Platelet-Derived Growth Factor (PDGF) and PDGF Receptor MRNAs in Skin Epithelial Cells and PDGF mRNA in Connective Tissue Fibroblasts. *Proc. Natl. Acad. Sci. U. S. A.* **1991**, *88* (2), 565–569.

(87) Ballaun, C.; Weninger, W.; Uthman, A.; Weich, H.; Tschachler, E. Human Keratinocytes Express the Three Major Splice Forms of Vascular Endothelial Growth Factor. *J. Invest. Dermatol.* **1995**, *104* (1), 7–10.

(88) Aldemir Dikici, B.; Reilly, G. C.; Claeysens, F. Boosting the Osteogenic and Angiogenic Performance of Multiscale Porous Polycaprolactone Scaffolds by in Vitro Generated Extracellular Matrix Decoration. *ACS Appl. Mater. Interfaces* **2020**, *12* (11), 12510–12524.

(89) Dikici, S.; Claeysens, F.; MacNeil, S. Decellularised Baby Spinach Leaves and Their Potential Use in Tissue Engineering

Applications: Studying and Promoting Neovascularisation. *J. Biomater. Appl.* **2019**, *34* (4), 546–559.